AD_____

Award Number: W81XWH-10-2-0117

TITLE: Novel Interventions for Heat/Exercise Induced Sudden Death and Fatigue

PRINCIPAL INVESTIGATOR: Susan L. Hamilton, Ph.D.

CONTRACTING ORGANIZATION: Baylor College of Medicine
Houston, TX 77030-3498

REPORT DATE: October 2011

TYPE OF REPORT: Annual

PREPARED FOR: U.S. Army Medical Research and Materiel Command
Fort Detrick, Maryland 21702-5012

DISTRIBUTION STATEMENT: Approved for Public Release;
Distribution Unlimited

REPORT DOCUMENTATION PAGE

Form Approved
OMB No. 0704-0188

1. REPORT DATE	2. REPORT TYPE	3. DATES COVERED
October 2011	Annual	1 October 2010 – 30 September 2011

4. TITLE AND SUBTITLE

Novel Interventions for Heat/Exercise Induced Sudden Death and Fatigue

5a. CONTRACT NUMBER

5b. GRANT NUMBER
W81XWH-10-2-0117

5c. PROGRAM ELEMENT NUMBER

6. AUTHOR(S)

Susan L. Hamilton, Sheila M Muldoon ,John Capacchione , Nyamkhishig Sambuughin , Rolf Bunger

E-Mail: susanh@bcm.edu

5d. PROJECT NUMBER

5e. TASK NUMBER

5f. WORK UNIT NUMBER

7. PERFORMING ORGANIZATION NAME(S) AND ADDRESS(ES)

Baylor College of Medicine
Houston, TX 77030-3498

8. PERFORMING ORGANIZATION REPORT NUMBER

9. SPONSORING / MONITORING AGENCY NAME(S) AND ADDRESS(ES)
U.S. Army Medical Research and Materiel Command
Fort Detrick, Maryland 21702-5012

10. SPONSOR/MONITOR'S ACRONYM(S)

11. SPONSOR/MONITOR'S REPORT NUMBER(S)

12. DISTRIBUTION / AVAILABILITY STATEMENT
Approved for Public Release; Distribution Unlimited

13. SUPPLEMENTARY NOTES

14. ABSTRACT
The goals are 1) to indentify RYR1 mutations associated with enhanced susceptibility to EHS/ER/MH by enrolling subjects diagnosed with these conditions and performing genetic screening. 2) to determine the mechanism of action of aminoimidazole carboxamide ribonucleotide (AICAR) and A769662 compound and test their suitability as interventions to prevent heat induced deaths in the porcine MH models. During the project period, 10 individuals were enrolled. RYR1 mutations/variants were identified in 5 of 10 enrolled subjects. Three of these mutations have been described as Malignant Hyperthermia (MH) causative mutations (Arg163Cys, Gly2434Arg and Arg2454Cys); one previously published MHS associated mutation, and one novel variant were identified in the RYR1 gene. Of the common mutations, the Arg2454Cys was identified in African American with positive CHCT results and a history of exertional rhabdomyolysis (ER). Identification of this mutation in a subject with ER further strengthens a link between MHS and ER. A new variant, Gly4820Arg, was found in a family with a history of death due to MHS and heat exertion. In the swine model of MH we compared the effectiveness of AICAR with dantrolene (2.4mgs/kg) in treatment of halothane triggered MH . Dantrolene was consistently effective, but AICAR 300,600 and -1200mgs/Kg was ineffective as a pre or post treatment for anesthetic induced MH. Consistent with this, AICAR prevents the heat induced deaths but not the anesthetic induced deaths in the mouse model of MH, suggesting different mechanisms. We demonstrate that AICAR prevents the heat response by preventing Ca2+ leak from RyR1.

15. SUBJECT TERMS
Exertional heat stroke, exertional rhabdomyolysis. Malignant hyperthermia Fatigue , AICAR , dantrolene, genetic analysis of type 1 ryanodine receptor (RYR1) Porcine Malignant hyperthermia model

16. SECURITY CLASSIFICATION OF:			17. LIMITATION OF ABSTRACT	18. NUMBER OF PAGES	19a. NAME OF RESPONSIBLE PERSON
a. REPORT	b. ABSTRACT	c. THIS PAGE			USAMRMC
U	U	U	UU	37	19b. TELEPHONE NUMBER *(include area code)*

Table of Contents

REPORT

Introduction: Exertional and/or environmental heat stroke (EHS) and exertional rhabdomyolysis (ER) has been reported in patients with diagnosis of Malignant Hyperthermia (MH). MH is a life-threatening pharmacogenetic disorder caused by mutations in the ryanodine receptor type 1gene *(RYR1)* encoding skeletal muscle calcium release channel. Our goals are 1) to indentify *RYR1* mutations associated with enhanced susceptibility to EHS/ER/MH by enrolling subjects diagnosed with these conditions and performing genetic screening. 2) to determine the mechanism of action of aminoimidazole carboxamide ribonucleotide (AICAR), 300, 600, and 1200 mg/kg and A769662 compound and test their suitability as interventions to prevent heat induced deaths in the porcine MH models.

Body: During the project period 10 individuals with a history of EHS/ER and MH were enrolled into this study. The RYR1 gene was screened in these individuals. The RYR1 mutations and variants were identified in 5 of 10 enrolled subjects (see Table 1 attached). Three well known disease causative mutations (Arg163Cys, Gly2434Arg and Arg2454Cys), one previously published MH associated mutation and one novel variant were identified in the RYR1 gene. Of the three common mutations, the Arg2454Cys was identified in an African American patient with positive CHCT results and a history of ER. The Arg2454Cys mutation has previously been reported in association with MH only (Robinson et al., 2006). Identification of this mutation in a subject with ER further strengthens a link between MH and ER. A new variant, Gly4820Arg, was found in a family with a history of death due to MH like event and heat exertion. We used 10 MHS animals with a single point mutation in the RYR1 (R615C) to compare the efficacy of AICAR 300-1200mg/kg and A769662 to Dantrolene. Yorkshire pigs that did not have the RyR1 genetic defect were used as controls. Future studies will be performed to determine if AICAR will be effective in a heat induced MH as it was reported in studies sung a mouse model.

In our second specific aim we proposed to develop interventions to prevent heat induced sudden death associated with RyR1 mutations. Task 2 was to elucidate the mechanism for AICAR's ability to prevent the environmenatl heat response (EHR). Task 2 and milestones 3 and 4 haves been completed. We are attaching a manuscript that is now in press at Nature Medicine (Lanner et al) demonstrating that AICAR prevents the heat induced death in our mouse model of EHR by decreasing Ca^{2+} leak via RyR1. The effects of acute doses of AICAR have been defined. In the coming year we will assess the effects of chronic doses.

Key Research Accomplishments:

- The RYR1 mutations and variants were identified in 5 of 10 enrolled subjects.
- These include: three well known disease causative mutations, Arg163Cys, Gly2434Arg and Arg2454Cys, a previously published MH associated mutation, Asp3986Glu, and a novel, Gly4820Arg, variant.
- AICAR was not effective in the treatment of anesthetic induced MH in a swine model.
- Dantrolene was effective in the treatment of swine induced maligant hyperthermia
- AICAR was shown to decrease Ca2+ leak from RYR1
- AICAR was shown to be effective in preventing heat induced death but not anesthethetic dinduced death in the mouse model of MH, suggesting that the two conditions have different underlying causes.

Reportable Outcomes: Manuscript in review : Hyperthermia and succinylcholine followed by Death

References:

Robinson RL, Carpenter D, Shaw M, Halsall J, Hopkins P. Mutations in *RYR1* in Malignant Hyperthermia and Central Core Disease. Hum Mutat 2006; 27:977-89.

Lanner, J., Georgiou, D., Dagnino-Acosta, A., Ainbinder, A., Cheng, Q., Joshi, A., Chen, Z., Yarotskyy, V., Oakes, J., Lee, C.-S., Monroe, T., Santillan, A., Dong, K., Goodyear, L., Ismailov, I., Rodney, G., Dirksen,R.,

and Hamilton, S.L. AICAR Prevents Heat Induced Sudden Death in RyR1 Mutant Mice Independent of AMPK Activation, Nature Medicine, in press.

Table 1. Results of RYR1 gene screening in enrolled subjects

SAMPLE ID	CLINICAL HISTORY	CONTRACTURE TEST RESULTS	FAMILY MEMBERS*	RESULTS OF GENETIC SCREENING
BU-01	REPEATED EXERCISE INDUCED RHABDOMYOLYSIS	N/A	N/A	IN PROGRESS
BU-02	HEAT RELATED DEATH IN A FAMILY MEMBER	N/A	5	IN PROGRESS
BU-03	EXERCISE INDUCED RHABDOMYOLYSIS, HEAT RELATED DEATH IN A FAMILY MEMBER	POSITIVE	4	Gly4820Arg
BU-04	POST MH MUSCLE PAIN WITH EXERCISE	POSITIVE	N/A	ARG163CYS
BU-05	EXERCISE INDUCED RHABDOMYOLYSIS, MH	POSITIVE	2	IN PROGRESS
BU-06	EXERCISE AND HEAT INTOLERANCE, MUSCLE CRAMPING AND MH	POSITIVE	4	Asp3986Glu
BU-07	REPEATED EXERCISE INDUCED RHABDOMYOLYSIS	POSITIVE	2	ARG2454CYS
BU-08	REPEATED EXERCISE INDUCED RHABDOMYOLYSIS	N/A	N/A	Gly2434Arg
BU-09	MH, EXERCISE AND HEAT INTOLERANCE	POSITIVE	N/A	In progress
BU-10	DEATH DUE TO MH LIKE EVENT	N/A	N/A	In progress

*Family members agreed to participate and will be enrolled into the study during the next quarter.

CONCLUSION: During this first year of the grant we have obtained data both in the mouse model and in humans to show that RyR1 mutations underlie an enhanced susceptibility to heat illness. We have also defined the mechanism by which AICAR prevents theis response in mice.

AICAR Prevents Heat Induced Sudden Death in RyR1 Mutant Mice Independent of AMPK Activation

Johanna T. Lanner[1*], Dimitra K. Georgiou[1*], Adan Dagnino-Acosta[1], Alina Ainbinder[2], Qing Cheng[1], Aditya D. Joshi[1], Zanwen Chen[1], Viktor Yarotskyy[2], Joshua M. Oakes[1], Chang Seok Lee[1],Tanner O. Monroe[1], Arturo Santillan[1], Keke Dong[1], Laurie Goodyear[3], Iskander I. Ismailov[1], George G. Rodney[1], Robert T. Dirksen[2], and Susan L. Hamilton[1#]

[1]Department of Molecular Physiology and Biophysics
Baylor College of Medicine
One Baylor Plaza, Houston, Texas 77030

[2]Department of Pharmacology and Physiology
University of Rochester Medical Center
601 Elmwood Avenue, Rochester, NY 14642

[3]Joslin Diabetes Center
Research Division
One Joslin Place
Boston, MA 02215

[*]The first two authors contributed equally to this manuscript
[#] All correspondence should be sent to Susan Hamilton, susanh@bcm.edu

Abstract.
Mice with a knock-in mutation (Y524S) in the type I ryanodine receptor (RyR1) die when exposed to short periods of temperature elevation (≥ 37 °C). We demonstrate that treatment with 5-aminoimidazole-4-carboxamide ribonucleoside (AICAR) prevents heat-induced sudden death in Y524S mice. The AICAR protection is independent of AMPK activation and results from a newly identified action on the mutant RyR1 to reduce Ca^{2+} leak, preventing Ca^{2+} dependent increases in both reactive oxygen and reactive nitrogen species that act to further increase resting Ca^{2+} concentrations. If unchecked, the temperature driven increases in resting Ca^{2+} and ROS/RNS create an amplifying cycle that ultimately triggers sustained muscle contractions, rhabdomyolysis and death. Although antioxidants are effective in reducing this cycle *in vitro*, only AICAR prevents the heat induced death *in vivo*. Our findings suggest that AICAR is likely to be effective in prophylactic treatment of humans with enhanced susceptibility to exercise/heat-induced sudden death associated with RyR1 mutations.

Introduction
An alarming increase in the number of exertional heat-related deaths among young, physically fit athletes, soldiers, policemen, and even individuals conducting normal "everyday" activities (e.g. yard work, home maintenance) are reported each year in the mainstream media, raising questions as to whether some individuals are more susceptible to heat and exercise-induced sudden death than others in the population. Recent findings suggest that at least 13 mutations in the skeletal muscle Ca^{2+} release channel (ryanodine receptor 1, RyR1) are associated with life-threatening responses to exertion, heat challenge and febrile illness [1-12]. RyR1 associated disorders are not rare; the prevalence of genetic abnormalities in the *RYR1* gene has been suggested to be as great as one in 3,000 individuals [7]. Mutations in RyR1 are associated with a wide spectrum of human muscle disorders (for review see, [13]) including malignant hyperthermia (MH), central core disease (CCD), multiminicore disease, core-rod myopathy, atypical periodic paralysis, neonatal hypotonia, idiopathic hyperCKaemia, late-onset axial myopathy, and congenital neuromuscular disease with uniform type 1 fibers.

The life threatening responses to elevated environmental temperatures associated with some RyR1 mutations (which we designate the enhanced heat response, EHR) display many similarities to heat stroke. Although sudden death in response to exertion, stress and/or high environmental temperature in young, apparently fit, adults can arise from pre-existing cardiac abnormalities [14] or the acute onset of organ failure (e.g., heart, kidney, liver) [15], it could also arise from organ failure secondary to rhabdomyolysis of skeletal muscle, triggered by exercise induced increases in body temperature. Dantrolene is an effective treatment to reverse anesthetic-induced MH episodes, but there are no FDA approved interventions for the other RyR1 myopathies. Given the severity and life threatening nature of some of the RyR1 myopathies, drugs that can be used prophylactically are greatly needed.

We created a mouse model [16, 17] by knocking-in a Y522S (Y524S in mice) mutation in RyR1 associated with MH in humans [18]. The heterozygous mice ($RyR1^{Y524S/WT}$ or

YS) demonstrate typical hallmarks of MH (e.g. whole body contractures, elevated core temperature, rhabdomyolysis and death) upon exposure to inhalation anesthetics [16]. These mice also display an enhanced susceptibility to a heat stroke-like response leading to sudden death when exposed to elevated environmental temperatures (>37 °C) or when exercising under warm (>25 °C) conditions [16]. In our search for agents that improve the myopathy [19] in these mice, we found that AICAR protected the mice against EHR. AICAR is an activator of the AMP-activated protein kinase (AMPK), a kinase that functions as a cellular energy sensor that is activated by increases in the AMP to ATP ratio [20]. AICAR is converted to 5-aminoimidazole-4-carboxamide ribonucleoside (ZMP) in the cell where it mimics AMP to activate AMPK and improves muscle endurance without exercise [21-24]. AMP binding to AMPK increases its phosphorylation at threonine 173, leading to prolonged activation. We now report that acute AICAR treatment prevents the EHR in YS mice, at least partially by directly inhibiting RyR1 Ca^{2+} leak and reducing oxidative/nitrosative stress.

RESULTS

AICAR prevents heat-induced sudden death in the YS mice. YS mice, if untreated, die after exposure to 37 °C for longer than 15 min [17]. This heat-induced death is prevented by acute administration of AICAR (600 mg kg^{-1} body weight) (**Fig. 1**). Administration of the same dose of AICAR after the onset of the heat-induced muscle contractures prevented death in 4 out of 5 YS mice exposed to 37 °C. To more rigorously quantify the time course of the response to temperature and the protective effects of AICAR, we measured VO_2 intake during exposure to 37 °C (**Fig. 1a**). VO_2 consumption of untreated YS mice increased dramatically compared to wild type (WT) mice upon exposure to the elevated temperature and this increase was prevented by AICAR (**Fig. 1a**). The AICAR dose used for these experiments (600 mg kg^{-1} body weight) is a commonly used dose reported not to exhibit significant side-effects in acute or chronic studies in rodents [19, 21, 24, 25]. The half maximal dose for survival in heat challenged YS mice was approximately 165 mg kg^{-1} body weight (**Fig. 1b**). YS mice exposed to 37 °C also exhibited a corresponding increase in VCO_2 elimination (**Fig. 1c**) and the respiratory exchange ratio (RER), calculated from $VCO_{2eliminated}/VO_{2consumed}$, approached a value of 1 (**Fig. 1d**), suggesting a significant shift toward anaerobic carbohydrate metabolism [26, 27]. The 10 min exposure to 37 °C significantly increased both serum $[K^+]$ (**Fig. 1e**) and rectal temperature (**Fig. 1f**) in YS mice. Administration of AICAR opposed all these increases (**Fig.1 c–f**). Although YS mice also die upon exposure to volatile anesthetics, AICAR pretreatment (600 mg kg^{-1} body weight) did not prevent this (5 out of 5 mice), suggesting that either volatile anesthetics are a stronger trigger than heat or that the heat-induced mechanism is different than the anesthetic-induced response.

AICAR prevention of the EHR is not due to an increase in AMPK activity. To evaluate the role of AMPK activation in the rescue of the YS mice from the EHR, we modified the AMPK assay using the SAMS peptide (a modified peptide corresponding to sequence around the AMPK target site in rat acetyl-CoA carboxylase, HMRSAMSGLHLVKRR) for use in muscle homogenates (see Methods). To verify the

assay, we determined the V_{max} (the maximum velocity of the reaction) and the K_m (the substrate concentration that produces an initial velocity of reaction that is one-half of V_{max}) in homogenates of soleus and EDL muscles of heat challenged WT and YS mice (**Fig. 2a**). The calculated K_ms were not significantly different among muscle samples, but the V_{max} (**Fig. 2b**) was significantly higher in the EDL of YS mice, presumably due to ongoing muscle contractions in YS EDL muscles and activation of AMPK by phosphorylation (**Supplementary Fig. 1a–f**). Consistent with increased muscle contractions in YS mice (even in the absence of heat challenge) glycogen levels were depleted in both the soleus and EDL of YS mice compared to WT mice (**Supplementary Fig. 2**). Glycogen is an inhibitor of AMPK [28]. The values of AMPK activity obtained in this study are comparable or higher than those obtained in skeletal muscle in other laboratories [29, 30].

To assess the role of AMPK activation in AICAR rescue, we used WT, YS mice, and both WT and YS mice crossed with mice expressing a muscle specific dominant negative AMPKα_2 (DN) [29, 31]. Mice (WT, YS, WT/DN and YS/DN) were injected with either saline or AICAR and exposed to 37 °C for 10–15 min. Mice that displayed signs of EHR were euthanized at the onset of the involuntary sustained contractures (muscle rigidity, arched back and extended legs). The presence of DN APMKα_2 did not prevent AICAR protection of the EHR reponse of YS mice (**Fig.2c**). The mice were also screened for changes in inspired VO_2 during heat challenge (**Fig. 2d**, values at 10 min at 37 °C). Untreated YS and YS/DN mice displayed the classic muscle signs of the EHR and their VO_2 level was significantly elevated. The VO_2 of YS/DN mice was, however, lower than that of YS mice, suggesting that AMPK activity contributes to the increased metabolic of YS mice during heat challenge. VO_2 levels in both YS and YS/DN mice were decreased by AICAR. None of the RyR1 wild type mice (WT and WT/DN) or any of the mice (WT, YS, WT/DN, YS/DN) treated with AICAR displayed adverse reactions to elevated temperature. The lower VO_2 values of YS and YS/DN mice treated with AICAR correlated well with increased survival of the YS mice during the heat challenge.

To confirm that the AICAR rescue was not due to AMPK activation, we isolated and homogenized the EDL and soleus muscles of treated mice (**Fig. 2c,d**) and determined the initial rate (v_0) of phosphorylation of 150 μM SAMs peptide at both 23 °C (**Supplementary Fig. 1g**) and 37 °C (**Fig. 2e,f).** This brief, acute *in vivo* AICAR treatment did not significantly activate AMPK in either the EDL or soleus. Mice expressing the dominant negative AMPK (WT/DN and YS/DN) treated with AICAR displayed decreased AMPK activity in both the soleus and the EDL. Despite the lack of increase in AMPK activity, all of the mice treated with AICAR survived the heat challenge. We confirmed these findings (**Fig. 2e, f**) by western blot for pAMPK and AMPK (**Supplementary Fig. 1)**. We conclude that activation of AMPK is not responsible for the ability of AICAR to rescue the YS mice from the heat challenge. We also tested the effects of chronic AMPK activation arising from expression of mutant AMPKγ_1 subunit (a muscle-specific noncatalytic γ_1 subunit mutant (R70Qγ) of AMPK) [32] and found that while AMPK activity was increased in muscle from these mice, this did not rescue YS mice exposed to 37 °C (designated YS/CA **Supplementary Fig. 1)**.

AICAR inhibits the activity of RyR1 in the presence of AMP-PCP. Since AMPK activation is not involved in the mechanism by which AICAR rescues YS mice during heat challenge, we next determined if AICAR had a direct effect on RyR1. ATP is a known activator of RyRs, and other adenine nucleotides (ADP, AMP, cAMP, adenosine, and adenine) function as weak partial agonists [33-35]. Since AICAR is a precursor of ZMP, it may also interact with RyR1 at the ATP binding site. We examined the effects of AICAR on [^{3}H]-ryanodine binding to sarcoplasmic reticulum membranes from WT and YS muscle. Ryanodine binds preferentially to the open state of RyR1, allowing [^{3}H]-ryanodine binding affinity to be used as an indirect measure of channel activation [16]. In the absence of ATP, AICAR produced a small concentration-dependent increase in [^{3}H]-ryanodine binding in both WT and YS membranes (**Fig. 3a**) and 1 mM AICAR produced a significant rightward shift in the concentration dependence of AMP-PCP (a nonhydrolyzable form of ATP) enhancement of [^{3}H]-ryanodine binding (**Fig. 3b,c**). We also examined the effects of AICAR on the Ca^{2+} dependence of [^{3}H]-ryanodine binding to membranes from WT and YS mice (**Supplementary Fig. 3a**). Ca^{2+} regulates RyR1 activity in a bimodal fashion with low Ca^{2+} concentrations (~1–10 μM) activating and high concentrations (~0.1–1 mM) inhibiting channel activity [17, 34, 35]. As previously reported [17], the Ca^{2+} enhancement of [^{3}H]ryanodine binding curve is left shifted for YS membranes compared to WT membranes. AICAR, however, does not alter the Ca^{2+} sensitivity of [^{3}H]-ryanodine binding, suggesting that AICAR does not prevent the EHR by decreasing the Ca^{2+} affinity of RyR1. AICAR had no effect on [^{35}S]FKBP12 binding or the caffeine sensitivity of [^{3}H]-ryanodine binding to sarcoplasmic reticulum membranes from either WT or YS mice or the caffeine sensitivity of sarcoplasmic reticulum Ca^{2+} release in *flexor digitorum brevis* (FDB) fibers (data not shown).

The inhibitory effect of AICAR on [^{3}H]-ryanodine binding suggests that the protective effect of AICAR could be due to a decrease in Ca^{2+} leak from mutant RyR1 channels at cellular concentrations of ATP. To test this possibility, we determined the effect of AICAR in the presence of 1 mM AMP-PCP on the single channel activity of WT and YS RyR channels reconstituted into planar lipid bilayers (**Fig. 3d,e**)**.** The RyR1 preparations were treated with the reducing agent, dithiothreitol, therefore, RyR1 was not reversibly oxidized or S-nitrosylated in these experiments. The channels from the heterozygous YS mice showed a variety of single channel behaviors (**Supplementary Fig. 4**), as expected for heteroligomer WT:YS tetramers. However, all YS and WT channels were inhibited by AICAR in the presence of AMP-PCP. AICAR significantly reduced the open probability (Po) of channels from YS mice (**Fig. 3f**), primarily by reducing the mean channel open time (**Fig. 3g**) with a small effect on closed times of WT channels (**Fig. 3h**). These findings demonstrate that AICAR reduces RyR1 channel activity in the presence of AMP-PCP.

AICAR prevents Ca^{2+} leak and ROS/RNS generation in YS myofibers. We explored the possibility that AICAR prevents temperature driven Ca^{2+} leak via RyR1. Representative Ca^{2+} transients elicited by 4-chloro-m-cresol (4-cmc, an activator of RyR1 Ca^{2+} release) were measured with Fura-2 in FDB fibers from WT and YS mice (**Supplementary Fig. 5**)**.** Treatment of FDB fibers with 1 mM AICAR for 10–20 min

decreased the magnitude of the temperature dependent increase in the resting Fura-2 ratio of FDB fibers from YS mice and prevented a decrease in the 4-cmc-induced "readily releasable RyR1 Ca^{2+} pool" (**Fig. 4a,b**). These findings are consistent with a role for AICAR in dampening RyR1 Ca^{2+} leak in the presence of cellular ATP. To assess the effects of AICAR on $Ca_v1.1$-RyR1 signaling during EC coupling, we determined the effect of 1 mM AICAR on L-type Ca^{2+} currents and voltage-gated sarcoplasmic reticulum Ca^{2+} release in WT myotubes in whole-cell voltage clamp experiments (**Supplementary Fig. 3b,c** and **Supplementary Table 1**). While pretreatment with 1 mM AICAR produced a modest increase in maximal L-type Ca^{2+} channel conductance, there was no effect of the drug on either the voltage dependence of this conductance or on the magnitude and voltage dependence of RyR1-mediated sarcoplasmic reticulum Ca^{2+} release (**Supplementary Fig. 3b,c** and **Supplementary Table 1**). Thus, we conclude that AICAR normalizes the enhanced Ca^{2+} leak properties of YS mutant RyR1 channels.

We used an *in situ* calibration to determine the magnitude of the temperature-dependent increase in resting myoplasmic Ca^{2+} concentration at 32 °C and 37 °C relative to 23 °C (**Fig. 4c,d).** The results indicate that the temperature-dependent increase in resting Ca^{2+} in YS FDB fibers was as high as 100–250 nM and 1 mM AICAR markedly reduced this increase in resting Ca^{2+}.

To determine if AICAR treatment impacts increased ROS and RNS production in fibers from YS mice, we assessed its effects on 4-amino-5-methylamino-2',7'-difluorofluorescein (DAF) and 5-carboxy-2',7'-dichlorodihydrofluorescein (DCF) fluorescence, respectively (**Fig. 4e,f**). The temperature dependent increases in both RNS and ROS in YS fibers were prevented by 1 mM AICAR (**Fig. 4e,f**).

Proteins in soleus and EDL muscles of YS mice exposed to physiological temperatures displayed increased levels of oxidative modifications (assessed with Oxyblots [36, 37]) which are reduced by 1 mM AICAR (**Fig. 4g–i**). The soleus of YS mice displayed increased oxidative stress even in mice not exposed to elevated temperatures and this increase was normalized by 1 mM AICAR (**Supplementary Fig. 6**). Since many proteins were found to be oxidatively modified in YS muscle exposed to heat, targets in addition to RyR1 may contribute to the EHR response.

NOS and NOX contribute to RyR1 Ca^{2+} leak. Both nitric oxide synthase isoforms eNOS and nNOS are activated by Ca^{2+} via calmodulin in skeletal muscle [38], suggesting that increases in myoplasmic Ca^{2+} are responsible for the observed increases in ROS and RNS production. The ability of ryanodine to block the temperature dependent increases in both DAF and DCF fluorescence supports this mechanism [17]. There are a number of potential sources of ROS production in muscle, including mitochondria, NADPH oxidases (NOX), and xanthine oxidase. A temperature-dependent increase in mitochondrial superoxide production in FDB fibers from YS mice was recently reported [39]. We tested gp91ds-TAT peptide to inhibit NOX [40], a scrambled gp peptide to control for nonspecific effects, and L-N^G-nitroarginine methyl ester (L-NAME) to inhibit NOS on the temperature dependent increases in DCF

fluorescence (**Fig. 5a,b**), DAF fluorescence (**Fig. 5c,d**), resting Ca^{2+} (**Fig. 5e,f**) and the peak Ca^{2+} release triggered by 4-cmc (**Fig. 5g,h**) in FDB fibers from YS mice. Inhibiting either NOX or NOS prevented the temperature dependent increases in both ROS and RNS in the YS fibers (**Fig. 5a–d**), suggesting that the major source of ROS in the YS muscle with heating is NOX (**Fig. 5a**). Blocking either RNS or ROS production decreased resting Ca^{2+} (**Fig. 5e,f**) and increased the magnitude of 4-cmc-induced Ca^{2+} release (**Fig. 5g,h**) in YS FDB fibers at 35 °C, supporting a feed forward cycle whereby Ca^{2+} increases RNS and ROS and, in turn, RNS and ROS increase RyR1 Ca^{2+} leak.

DISCUSSION

Mutations in RyR1 underlie a life-threatening sensitivity to heat and exercise in humans [2, 4, 5, 10, 11, 12, 41, 42]. Similar heat/exercise sensitivity is found in mice with the Y524S RyR1 knock-in mutation. We demonstrate that the YS mutation enhances RyR1 Ca^{2+} leak, especially at higher temperatures which, in turn, drives increased oxidative/nitrosative stress. Oxidative and nitrosative modifications of RyR1 and other muscle proteins result in a feed-forward cycle that drives both the myopathy and the EHR [17]. Several groups have suggested that Ca^{2+} influx may contribute to sustained Ca^{2+} increases associated with the MH response [43-46], but the possibilities that Ca^{2+} influx via stretch-, store-, or voltage-operated Ca^{2+} channels contributes to the EHR in the YS mice remains to be investigated.

There are no known drug interventions to prevent heat-induced death in humans. We demonstrate that AICAR, a compound that actually improves muscle performance [21-24], prevents heat-induced sudden death in YS mice. We also demonstrate that the ability of AICAR to protect these mice is not due to activation of the energy sensing kinase, AMPK, but rather to a direct inhibition of Ca^{2+} leak via RyR1, preventing heat-induced increases in resting Ca^{2+}, Ca^{2+} store depletion and increases in RNS and ROS production (**Fig. 6**). RyR1 is known to be activated by both oxidation [47] and *S*-nitrosylation [47], but AICAR inhibition of RyR1 Ca^{2+} leak does not depend on oxidation or *S*-nitrosylation of RyR1.

Despite the finding that ROS and RNS are involved in the feed forward cycle, antioxidants such as N-acetylcysteine, which blocks both ROS and RNS increases in YS myotubes and FDB fibers, delay but do not prevent heat-induced sudden death in YS mice [17]. This lack of *in vivo* efficacy most likely reflects limited bioavailability of antioxidants, which has been a drawback to antioxidant therapy for a number of diseases (for review see [48]). In contrast, AICAR, which actually improves muscle function with only very mild side effects, is 100% effective in preventing the heat-induced sudden death in the YS mice.

In summary, we demonstrate that AICAR interacts with RyR1 to decrease Ca^{2+} leak in the presence of cellular concentrations of ATP (a more efficacious agonist). AICAR rescues the EHR of YS mice at least partially by reducing RyR1 Ca^{2+} leak and oxidative/nitrosative stress to levels sufficient to disrupt the destructive feed-forward

cycle that, when unchecked, leads to sustained contractures, rhabdomyolysis and death. We propose the potential use of AICAR for prophylactic treatment in humans with enhanced susceptibility to exercise and /or heat-induced sudden death associated with RyR1 disease mutations.

ACKNOWLEDGEMENTS

This work was supported by grants from US National Institutes of Health (AR053349), the Department of Defense (DAMD W81XWH-10-2-0117) and the Muscular Dystrophy Association of America. JT Lanner was supported by a postdoc fellowship from The Swedish Research Council. A. Dagnino-Acosta was supported by a postdoctoral fellowship from CONACYT (150489). The model figure 6 was created by Scott A. Weldon, MA CMI.

Johanna T. Lanner designed, performed and analyzed experiments in Figure 1a and b, Figure 3a-c, analyzed data and supplemental Figure 1a-f. She wrote the initial draft of the paper, edited the final draft of the paper. Dimitra K. Georgiou developed the new AMPK assay and designed, performed and analyzed experiments for Fig 2. She also wrote an intermediate draft of the paper, prepared the supplemental section, and helped write and edit final draft of the manuscript. Adan Dagnino-Acosta designed, performed and analyzed the experiments in Fig. 4f and Fig. 5a and b. He also participated in the writing of the manuscript. Alina Ainbinder designed performed and analyzed data for Fig.4d. Qing Cheng made the initial AICAR discovery and performed the experiments in Figure 4a-f and supplemental Figure 2. Adi Joshi generated and analyzed the data in Figure 4g-l and supplemental Figure 6. Viktor Yarotskyy designed performed and analyzed data in supplemental Table 1 and supplemental figure analyzed data in supplemental Figure 3b and c. Chang Seok Lee designed, performed and analyzed data (western blots and qrtPCR) to demonstrate that calcium handling proteins are not changed by the YS mutation or by AICAR. Tanner Monroe designed experiments and performed and analyzed many of the pAMPK/AMPK western blots in supplemental Figure 1. Arturo Santillan performed all of the mouse dissections, tested endurance of mice on running wheels, performed IDC and contributed to the preparation of the manuscript. Keke Dong handled all matings and genotyping, performed IDC on mice and helped in manuccript preparation. Laurie Goodyear provided mice, advised on crucial metabolic experiments and AMPK assays and participated in writing and critique of the manuscript. Iskander Ismailov designed and performed experiments for Fig. 4a and b and 5a and b, helped in the analysis of the bilayer data and contributed to manuscript preparation and revision. George G. Rodney contributed reagents, supervised, designed and analyzed the experiments to assess the role of NOX in the response and contributed to manuscript preparation and revision. Robert T. Dirksen designed, supervised and analyzed all Ca^{2+} measurements, critiqued and analyzed all studies, and contributed to manuscript preparation and revision. Susan L. Hamilton supervised all experiments, reanalyzed all data for accuracy, plotted all figures and wrote the final draft of the manuscript. All authors reviewed and approved the final version of the manuscript.

The authors declare no competing financial interests.

METHODS

Animals. For the experiments involving animals we used 6–10 week old male heterozygous RyR1$^{Y524S/WT}$ knock-in (YS) mice and their wild-type (WT) littermates (on C57BL/6 background) [16]. We also crossed YS mice with transgenic mice that express either a muscle-specific constitutively active AMPK-$\gamma1^{R70Q}$ (CA) [32] or dominant negative AMPK-$\alpha2^{D157A}$ (DN) [29, 31]. We housed all mice at room temperature with a 12:12 hour light-dark cycle and we provided food and water *ab libitum*. We injected AICAR (Toronto Research Chemicals) and saline subcutaneously. Dose of AICAR was 600 mg Kg^{-1} of body weight, unless otherwise stated, and was administered 10 min prior to heat challenge. All procedures were approved by the Animal Care Committee at Baylor College of Medicine.

AMPK activity assay. We analyzed AMPK activity by assessing the incorporation of ^{32}P radiolabeled phosphate from ATP (PerkinElmer) into 150 μM SAMS (AnaSpec) peptide for 15 min at 37 °C as described in [49] with modifications. The assay was on 5 μg homogenates, 1 μM thapsigargin (Sigma-Aldrich) and 10 mM EGTA (Sigma).

Indirect calorimetry. We assessed O_2 consumption and CO_2 production of individual mice undergoing heat-challenge at 37 °C at 1 min intervals for up to a 15 min period as previously described [17]. We performed all metabolic experiments approximately at the same time per day (10:00–13.00) and mice were not fasted.

Serum K^+. We measured serum K^+ in the Center for Comparative Medicine at Baylor College of Medicine with a Roche COBAS INTEGRA 400 plus instrument according to the instructions of the manufacturer.

Radioligand binding. We performed equilibrium ^3H-ryanodine[17, 47] (5 nM) and ^{35}S-FKBP12[51] (20 nM) binding studies with skeletal muscle membranes as previously described.

Single channel recordings and analyses. We performed single channel measurements by fusing proteoliposomes containing purified RyR1 from skeletal muscles with lipid bilayers bathed in 250 mM Cs-HEPES (Sigma), pH 7.4 (cis-) and 50 mM Cs-methanesulphonate (CsMS, trans-) (Sigma) as previously described[50]. Free Ca^{2+} was ~6–8 μM, since neither Ca^{2+} nor EGTA were added. After single channel activity became evident in the presence of 1 mM AMP-PCP (Sigma) (both chambers), we adjusted CsMS in the trans chamber to 250 mM and we added 1 mM AICAR to both sides of the membrane. We recorded RyR1 currents at a holding potential of + 30 mV, digitally filtered at 2 KHz, and acquired at 10 KHz sampling rate using Clampex 10.0 (Molecular Devices). For illustration purposes, we digitally filtered the records shown at 300 Hz. We analyzed the recordings using Clampfit 10.0 (Molecular Devices).

We calculated open probability for each channel from the events analyses as a ratio of the total open time (sum of all open times, including partial openings of the channels to a sub-conductance state) by the total time of the record. We calculated mean open and closed times by fitting the dwell time histograms to a single exponential log probability function.

Oxyblot. We assessed oxidative stress with the OxyBlotTM Protein Oxidation Detection Kit (Millipore) in 10 μg soleus and EDL homogenates according to the protocol provided by the manufacturer.

Fiber isolation. We isolated and plated single fibers from the FDB muscles as previously described[52].

Measurements of ROS and RNS. To assess reactive oxygen and nitrogen species (ROS and RNS), we loaded the FDB fibers with 5-carboxy-2',7'-dichlorodihydrofluorescein (CM-H_2DCFDA, DCF) (Invitrogen) or 4-amino-5-methylamino-2',7'-difluorofluorescein (DAF-FM diacetate, DAF) (Invitrogen) dyes as described in[17]. Imaging details are described in Supplementary Methods. We also tested the effects of 1 mM AICAR, 50 μM L-NAME (Sigma), and 5 μM gp91ds-tat peptide or of the corresponding scrambled peptide[40](Biopolymer Core, University of Maryland) on DCF and DAF fluorescence following 1 h preincubation at room temperature.

Ca^{2+} measurements.
We measured resting Ca^{2+} and the readily-releasable RyR1 Ca^{2+} pool in single FDB fibers loaded with Fura-2AM (Invitrogen) by the means of conventional epifluorescence technique (details in Supplementary Methods).

Measurements of the temperature dependence of resting Ca^{2+}. Resting Fura-2 fluorescence ratios ($R=F_{340}/F_{380}$) were converted to free Ca^{2+} concentrations using an *in situ* calibration approach [14] and the following equation: $[Ca^{2+}]_I = K_d \cdot \beta \cdot [(R-R_{min})/(R_{max}-R)]$, where K_d is the Ca^{2+} affinity of Fura-2, β is the ratio of the 380 nm emission recorded under Ca^{2+} free and Ca^{2+} saturating conditions, R_{min} is the emission ratio under Ca^{2+} free conditions, and R_{max} is the emission ratio under Ca^{2+} saturating conditions. The values of β, R_{min}, and R_{max} were determined experimentally. The K_d used was taken from the *in vitro* calibration of Fura-2 in the presence of 27 mg ml^{-1} of aldolase (428 nM) [15] and was assumed to be independent of temperature in intact cells as demonstrated previously[53] (details in Supplementary Methods).

Statistical analyses. Data in figures are mean ± SEM. We performed the statistical analyses of two groups with Student's t-test. $P < 0.05$ is considered statistically significant, $*P < 0.05$, $**P < 0.01$, $***P < 0.001$.

FIGURE LEGENDS

Figure 1 Effect of AICAR on heat induced sudden death in YS mice heat challenged at 37 °C. (**a**) Oxygen consumption (VO_2) during a 15 min exposure of mice at 37 °C, (*n* = 3–9). (**b**) VO_2 and survival rate (%) of mice exposed to 37 °C as a function of AICAR dose, (*n* = 3–6). (**c**) CO_2 elimination (VCO_2) at the 10^{th} min of heat challenge. (**d**) Respiratory exchange ratio (RER), calculated as $VCO_{2eliminated}/VO_{2consumed}$ at the 10^{th} min of heat challenge. (**e**) Serum K^+ after 10 min exposure to heat. (**f**) Rectal temperature, measured immediately after 10 min exposure to heat. In panels c–f AICAR treatment is indicated with subscript A and *n* numbers are shown. **P* < 0.05, ***P* < 0.01, ****P* < 0.001.

Figure 2 AICAR rescue of the YS mice is independent of AMPK activation. (**a**) Initial phosphorylation rate of SAMS peptide in muscle homogenates. Solid lines represent hyperbolic fits ($\nu 0=(V_{max}*[SAMS])/(K_m+[SAMS])$). Km values are: 145 ± 38 μM (*n* = 4) for WT soleus, 120 ± 44 μM (*n* = 3) for YS soleus; 137 ± 37 μM (*n* = 3) for WT EDL and 149 ± 36 μM (*n* = 3) for YS EDL. (**b**) Maximum phosphorylation rate (Vmax) of SAMS peptide in muscle homogenates of soleus (sol) and EDL. (**c**) Cumulative summary of % of mice of each genotype and treatment that undergo EHR and (**d)** correspondent VO_2 consumption at the 10^{th} min of heat challenge at 37 °C. (**e**) AMPK activity in soleus and (**f**) in EDL muscle of mice exposed to 37 °C. AICAR treatment, in panels e–h, is indicated with subscript A, and *n* numbers are shown in panels d–h. **P* < 0.05, ***P* < 0.01, ****P* < 0.001.

Figure 3 Effect of AICAR on RyR1 in the presence of AMP-PCP. (**a**) Representative plots of ^{3}H-ryanodine binding to WT and YS sarcoplasmic reticulum membranes with increasing AICAR concentrations in the absence of AMP-PCP. (**b**) Representative plots of ^{3}H-ryanodine binding to WT sarcoplasmic reticulum membranes with increasing concentrations of AMP-PCP in the absence or presence(+A) of 1 mM AICAR. EC_{50} values: WT 100 ± 5 μM, (*n* = 3); WT + A 318 ± 51 μM, (*n* = 3), *P* < 0.001. (**c**) Representative plots of ^{3}H-ryanodine binding to YS sarcoplasmic reticulum membranes with increasing concentrations of AMP-PCP in the absence or presence(+A) of 1 mM AICAR. EC_{50} values: YS 153 ± 5 μM; YS+A 330 ± 27 μM, (*n* = 3), *P* < 0.01. EC_{50} values represent the mean of three independent preparations. (**d**) Representative single channel recordings of WT RyR1 in the presence of 1 mM AMP-PCP, before and after addition of 1 mM AICAR. (**e**) One subclass of single YS RyR1 channels (others in **Supplementary Fig. 4**) in the presence of 1 mM AMP-PCP, before and after 1 mM AICAR. (**f**) RyR1 probability of opening (P_O), (**g**) mean channel open time (τ_{open}) and (**h**) mean channel closed time (τ_{closed}) for the WT and YS channels. AICAR treatment is indicated with the subscript A, and *n* numbers are indicated in panels f–h. ****P* < 0.001.

Figure 4 Effect of AICAR on Ca^{2+}, ROS and RNS in single isolated WT and YS FDB fibers. (**a**) Peak of Ca^{2+} transient triggered by *in vitro* application of 4-cmc. (**b**) Resting cytosolic Ca^{2+} in indicated fibers. (**c**) Representative images of single fibers loaded with Fura-2AM. Scale bars represent 20 μm. Vertical linear scales represent free [Ca^{2+}] 0–1.7 μM (**d**) Estimation of the changes in resting Ca^{2+} (nM) with temperature. *In vitro* AICAR treatment is indicated (+A), (*n* = 4–6). (**e**) DAF fluorescence ratio as a measure

of RNS production and (**f**) DCF fluorescence ratio as a measure of ROS production, in FDB fibers. (**g**) Representative Oxyblot (top) and Coomassie stained gel (bottom) to assess oxidative stress by immunodetection of carbonyl groups (anti-DNP, green) normalized to a non specific band (red) in WT (W) and YS (Y) muscle homogenates. Mice were injected either with saline (-) or AICAR(+) and were heat challenged at 37 °C (+) or not (-) (**h**) Oxidative stress in soleus and (**i**) EDL muscle homogenates, as quantified by Oxyblot densitometry. *In vitro* AICAR application is indicated with subscript A in panels a, b, e, f, h and i, and *n* numbers are also indicated. **P* < 0.05, ***P* < 0.01, ****P* < 0.001.

Figure 5 Effects of NOX or NOS inhibition in single isolated FDB fibers at 35 °C. WT and YS fibers were preincubated either with the NOX inhibitor gp91ds-tat peptide (gp) using the corresponding scrambled peptide as control (gps), or the NOS blocker L-NAME (L), blockers are shown as subscripts. DCF fluorescence ratio as a measure of ROS production in fibers incubated with (**a**) gp91ds-tat peptide or the control peptide and (**b**) L-NAME. DAF fluorescence ratio as a measure of RNS production, in fibers incubated with (**c**) gp91ds-tat peptide or the control peptide and (**d**) L-NAME. Fura-2 ratio as a measure of resting Ca^{2+} in fibers incubated with (**e**) gp91ds-tat peptide or the control peptide and (**f**) L-NAME. Fura-2 ratio as a measure of Ca^{2+} transient peak triggered by *in vitro* application of 4-cmc in fibers incubated with (**g**) gp91ds-tat peptide or the control peptide and (**h**) L-NAME. The *n* numbers are indicated in all panels. **P* < 0.05, ***P* < 0.01, ****P* < 0.001.

Figure 6 Model for the AICAR prevention of EHR. We are proposing that the heat induced sudden death or EHR in the YS mice arises from a mutation in RyR1 that increases Ca^{2+} leak at elevated temperatures. The increased cytosolic Ca^{2+} activates NOX (and to a lesser extent mitochondria) and NOS to produce ROS and RNS, respectively. Both ROS and RNS modify RYR1, and other skeletal muscle proteins to further increase the temperature dependent Ca^{2+} leak, promoting a feed forward cycle that eventually results in sustained contractures and death. AICAR binds directly to RyR1 to inhibit Ca^{2+} leak in the presence of cellular concentrations of ATP. Decreased Ca^{2+} leak prevents ROS and RNS overproduction and stops the feed forward cycle. A role for Ca^{2+} influx either via $Ca_V1.1$, stretch or store operated channels remains to be investigated.

Literature Cited

1. Bouchama, A., and Knochel, J. P., *Heat Stroke.* N Engl J Med, 2002. **346**(25): p. 1978-88.
2. Hopkins, P.M., Ellis, F.R. and Halsall, P.J. , *Evidence for related myopathies in exertional heat stroke and malignant hyperthermia.* The Lancet, 1991. **338**: p. 1491-92.
3. Jurkat-Rott, K., McCarthy, T., and Lehmann-Horn, F., *Genetics and Pathogenesis of Malignant Hyperthermia.* Muscle Nerve, 2000. **23**(1): p. 4-17.

4. Wappler, F., Fiege, M., Steinfath, M., Agarwal, K., Scholz, J., Singh, S., Matschke, J., and Schulte Am Esch, J., *Evidence for Susceptibility to Malignant Hyperthermia in Patients with Exercise-Induced Rhabdomyolysis.* Anesthesiology, 2001. **94**(1): p. 95-100.
5. Davis, M., Brown, R., Dickson, A., Horton, H., James, D., Laing, N., Marston, R., Norgate, M., Perlman, D., Pollock, N., and Stonwell, K., *Malignant Hyperthermia Associated with Exercise-Induced Rhabdomyolysis or Congenital Abnormalities and a Novel RYR1 Mutation in New Zealand and Australian Pedigrees.* Br J Anaesth, 2002. **88**(4): p. 508-15.
6. Treves, S., Anderson, A. A., Ducreux, S., Divet, A., Bleunven, C., Grasso, C., Paesante, S., and Zorzato, F., *Ryanodine Receptor 1 Mutations, Dysregulation of Calcium Homeostasis and Neuromuscular Disorders.* Neuromuscul Disord, 2005. **15**(9-10): p. 577-87.
7. Rosenberg, H., Davis, M., James, D., Pollock, N. & Stowell, K, *Malignant hyperthermia.* Orphanet J Rare Dis 2007. **2**(21).
8. Lanner, J.T., Georgiou, D.K., Joshi, A.D. and Hamilton, S.L. , *Ryanodine Receptors: structure, expression, molecular details, and function in calcium release. .* Cold Spring Harb Pespect Bio, 2010. **2**(11).
9. Larach, M.G., Gronert, G.A., Allen, G.C.M.D., Brandom, B.W.M.D. and Lehman, E.B.M.S., *Clinical presentation, treatment, and complications of malignant hyperthermia in North America from 1987 to 2006.* Anesth Analg, 2010. **110**: p. 498-507.
10. Capacchione, J.F.a.M., S.M, *The relationship between exertional heat illness, exertional rhabdomyolysis, and malignant hyperthermia.* Anesth Analg, 2009. **109**: p. 1065-1069.
11. Groom, L., Muldoon, S.M., Tang, Z.Z., Brandon, B.W., Bayarsaikhan, M., Bina, S., Lee, H-S, Sambuughin, N., and Dirksen, R.T., *Identical de novo mutation in the type I ryanodine receptor gene associated with fatal, stress-induced malignant hyperthermia in two unrelated families.* Anesthes, 2011, in press.
12. Vladutiu, G.D., Isackson, P.J., Kaufman, K., Harley, J.B., Cobb, B., Christopher-Stine, L., and Wortmann, R.L., *Genetic risk for malignant hyperthermia in non-anesthesia-induced myopathies.* Mol Genet Metab, 2011.
13. Mackrill, J.J., *Ryanodine receptor calcium channels and their partners as drug targets.* Biochem Pharmacol, 2010. **79**(11): p. 1535-43.
14. Grynkiewicz, G., Poenie, M., and Tsien, R.Y., *A new generation of Ca2+ indicators with greatly improved fluorescence properties.* J Biol Chem, 1985. **260**(6): p. 3440-3450.
15. Konishi, M., Olson, A., Hollingworth, S., and Baylor, S.M., *Myoplasmic binding of fura-2 investigated by steady-state fluorescence and absorbance measurements.* Biophys J, 1988. **54**(6): p. 1089-104.
16. Chelu, M.G., Goonasekera, S. A., Durham, W. J., Tang, W., Lueck, J. D., Riehl, J., Pessah, I. N., Zhang, P., Bhattacharjee, M. B., Dirksen, R. T., and Hamilton, S. L., *Heat- and Anesthesia-Induced Malignant Hyperthermia in an RyR1 Knock-In Mouse.* FASEB J, 2006. **20**(2): p. 329-30.

17. Durham, W.J., Aracena-Parks, P., Long, C., Rossi, A. E., Goonasekera, S. A., Boncompagni, S., Galvan, D. L., Gilman, C. P., Baker, M. R., Shirokova, N., Protasi, F., Dirksen, R., and Hamilton, S. L., *RyR1 S-Nitrosylation Underlies Environmental Heat Stroke and Sudden Death in Y522S RyR1 Knockin Mice.* Cell, 2008. **133**(1): p. 53-65.
18. Quane, K.A., Keating, K. E., Healy, J. M., Manning, B. M., Krivosic-Horber, R., Krivosic, I., Monnier, N., Lunardi, J., and McCarthy, T. V., *Mutation Screening of the RYR1 Gene in Malignant Hypertherima: Detection of a Novel Tyr to Ser Mutation in a Pedigree with Associated Central Core.* Genomics, 1994. **23**(1): p. 236-9.
19. Boncompagni, S., Rossi, A.E., Micaroni, M., Hamilton, S.L., DIrksen, R.T., Franzini-Armstrong, C., and and Protasi, F., *Characterization and temporal development of cores in a mouse model of malignant hyperthermi.* Proc Natl Acad Sci USA, 2009. **106**(51): p. 21996-22001.
20. Corton, J.M., Gillespie, J.G., Hawley, S.A., and Hardie, D.G., *5-Aminoimidazole-4-Carboxamide Ribonucleoside: A Specific Method for Activating AMP-Activated Protein Kinase in Intact Cells?* Eur J Biochem, 1995. **229**(2): p. 558-565.
21. Narkar, V.A., Downes, M. Yu, R.T., Embler, E., Wang, Y.X., Banayo, E., Mihaylova, M.M., Nelson, M.C., Zou, Y., Juguilon, H., Kang, H., Shaw, R.J., and Evans, R.M., *AMPK and PPARdelta agonists are exercise mimetics.* Cell, 2008. **134**(3): p. 405-15.
22. Holmes, B.F., Kurth-Kraczek, E.J. and Winder, W.W. , *Chronic activation of 5'-AMP-activated protein kinase increases GLUT-4, hexokinase, and glycogen in muscle.* J Appl Physiol, 1999. **87**: p. 1990-1995.
23. Pold, R., Jensen, L.S., Jessen, N., Buhl, E.S., Schmitz, O., Flyvbjerg, A., Fujii, N., Goodyear, L.J., Gotfredsen, C.F., Brand, C.L., and Lund, S., *Long-Term AICAR Administration and Exercise Prevents Diabetes in ZDF Rats.* Diabetes, 2005. **54**: p. 928-934.
24. Winder, W.W., Holmes, B.F., Rubink, D.S., Jensen, E.B., Chen, M., and Holloszy, J.O., *Activation of AMP-activated protein kinase increases mitochondrial enzymes in skeletal muscle.* J Appl Physiol, 2000. **88**(6): p. 2219-26.
25. Jørgensen, S.B., Treebak, J.T., Viollet, B., Schjerling, P., Vaulont, S., Wojtaszewski, J.F., and Richter, E.A., *Role of AMPKalpha2 in basal, training-, and AICAR-induced GLUT4, hexokinase II, and mitochondrial protein expression in mouse muscle.* Am J Physiol Endocrinol Metab, 2007. **292**(1): p. E331-E339.
26. Wasserman, K., Beaver, W.L. and Whipp, B.J. , *Gas exchange theory and the lactic acidosis (anaerobic) threshold.* Circulation, 1990. **81**(Supp II): p. 14-30.
27. Solberg, G., Robstad, B., Skjønsberg, O.H. and Borchseniu, F, *Respiratory gas exchange indices for estimating the anaerobic threshold.* J Sports Sci Med, 2005. **4**: p. 29-36.
28. McBride, A., Ghilagaber, S., Nikolaev, A., and Hardie, D.G., *The glycogen-binding domain on the AMPK beta subunit allows the kinase to act as a glycogen sensor.* Cell Metab, 2009. **9**(1): p. 23-24.

29. Fujii, N., Hirshman, M.F., Kane, E.M., Ho, R.C., Peter, L.E., Seifert, M.M., and Goodyear, L.J., *AMP-activated protein kinase alpha2 activity is not essential for contraction- and hyperosmolarity-induced glucose transport in skeletal muscle.* J Biol Chem, 2005. **280**(47): p. 39033-41.
30. Tadaishi, M., Miura, S., Kai, Y., Kawasaki, E., Koshinaka, K., Kawanaka, K., Nagata, J., Oishi, Y., and Ezaki, O., *Effect of exercise intensity and AICAR on isoform-specific expressions of murine skeletal muscle PGC-1α mRNA: a role of β_2-adrenergic receptor activation.* Am J Physiol Endocrinol Metab, 2011. **300**(2): p. E341-9.
31. Fujii, N., Ho, R.C., Manabe, Y., Jessen, N., Toyoda, T., Holland, W.L., Summers, S.A., Hirshman, M.F., and Goodyear, L.J., *Ablation of AMP-activated protein kinase alpha2 activity exacerbates insulin resistance induced by high-fat feeding of mice.* Diabetes, 2008. **57**(11): p. 2958-2966.
32. Barre, L., C. Richardson, M. Hirshman, J. Brozinick, S. Fiering, B. Kemp, Goodyear, L.J., and Witters, L.A., *Genetic Model for the Chronic Activation of Skeletal Muscle AMP-Activated Protein Kinas Leads to Glycogen Accumulation.* Am J Physiol, Endo, Meta, 2007. **292**(3): p. E802-E811.
33. Meissner, G., *Adenine nucleotide stimulation of Ca2+-induced Ca2+ release in sarcoplasmic reticulum.* J Biol Chem, 1984. **259**: p. 2365-2374.
34. Meissner, G., Rios, E., Tripathy, A. and Pasek, D.A., *Kinetics of rapid calcium release by sarcoplasmic reticulum. Effects of calcium, magnesium, and adenine nucleotides.* Biochemistry, 1986. **25**: p. 236-244.
35. Meissner, G., Rios, E., Tripathy, A., and Pasek, D. A., *Regulation of Skeletal Muscle Ca2+ Release Channel (Ryanodine Receptor) by Ca^{2+} and Monovalent Cations and Anions.* J Biol Chem, 1997. **272**(3): p. 1628-38.
36. Terracciano, C., Nogalska, A., Engel, W.K., Wojcik, S. and Askanas, V, *In inclusion-body myositis muscle fibers Parkinson-associated DJ-1 is increased and oxidized.* Free Radic Biol Med, 2008. **45**(6): p. 773-779.
37. Korolainen, M.A., Goldsteins, G., Nyman, T.A., Alafuzoff, I., Koistinaho, J., and Pirttilä, T., *Oxidative modification of proteins in the frontal cortex of Alzheimer's disease brain.* Neurobiol Aging, 2006. **27**(1): p. 42-53.
38. Stamler, J.S., and Meissner, G., *Physiology of nitric oxide in skeletal muscle.* Physiol Rev, 2001. **81**(1): p. 209-237.
39. Wei, L., Salahura, G., Boncompagni, S., Kasischke, K.A., Protasi, F., Sheu, S., and Dirksen, R.T., *Mitochondrial superoxide flashes: metabolic biomarkers of skeletal muscle activity and disease.* FASEB, 2011.
40. Rey, F.E., Cifuentes, M.E., Kiarash, A., Quinn, M.T., and Pagano, P.J., *Novel competitive inhibitor of NAD(P)H oxidase assembly attenuates vascular O(2)(-) and systolic blood pressure in mice.* Circ Res, 2001. **89**(5): p. 408-414.
41. Tobin JR, J.D., Challa VR, Nelson TE, Sambuughin N., *Malignant hyperthermia and apparent heat stroke.* JAMA, 2001. **286**(2): p. 168-9.
42. Nishio, H., Sato, T., Fukunishi, S., Tamura, A., Iwata, M., Tsuboi, K., and Suzuki, K., *Identification of malignant hyperthermia-susceptible ryanodine receptor type 1 gene (RYR1) mutations in a child who died in a car after exposure to a high environmental temperature.* Leg Med (Tokyo), 2009. **11**(3): p. 142-3.

43. Rock, E.a.K.-R., G., *Effect of halothane on the Ca2+-transport system of surface membranes isolated from normal and malignant hyperthermia pig skeletal muscle.* Archives of Biochemistry and Biophysics, 1987. **256**(2): p. 703-707.
44. Duke, A.M., Hopkins, P.M., Calaghan, S.C., Halsall, J.P., and Steele, D.S., *Store-operated Ca2+ entry in malignant hyperthermia-susceptible human skeletal muscle.* J Biol Chem, 2010. **285**(33): p. 25645-53.
45. Williams, J.H., Holland, M., Lee, J.C., Ward, C.W., and McGrath, C.J., *BAY K 8644 and nifedipine alter halothane but not caffeine contractures of malignant hyperthermic muscle fibers.* Am J Physiol, 1991. **261**(4 pt 2): p. R782-786.
46. Pirone, A., Schredelseker, J., Tuluc, P., Gravino, E., Fortunato, G., Flucher, B.E., Carsana, A., Salvatore, F., and Grabner, M., *Identification and functional characterization of malignant hyperthermia mutation T1354S in the outer pore of the Cavalpha1S-subunit.* Am J Physiol Cell Physiol., 2010. **299**(6): p. C1345-54.
47. Aracena-Parks, P., Goonasekera, S. A., Gilman, C. P., Dirksen, R. T., Hidalgo, C., and Hamilton, S. L., *Identification of Cysteines Involved in S-Nitrosylation, S-Glutathionylation, and Oxidation to Disulfides in Ryanodine Receptor Type 1.* J Biol Chem, 2006. **281**(52): p. 40354-68.
48. Firuzi, O., Miri, R., Tavakkoli, M., and Saso, L., *Antioxidant Therapy: Current Status and Future Prospects.* Curr Med Chem, 2011. **Epub ahead of print**.
49. Winder, W., and Hardie, D.G., *Inactivation of acetyl-CoA carboxylase and activation of AMP-activated protein kinase in muscle during exercise.* Am J Physiol, 1996. **270**(2 pt 1): p. E299-304.
50. Lee, H.B., Xu, L. and Meissner, G, *Reconstitution of the skeletal muscle ryanodine receptor-Ca2+ release channel protein complex into proteoliposomes.* J Biol Chem, 1994. **269**(18): p. 13305-13312.
51. Aracena, P., Tang, W., Hamilton, S. L., and Hidalgo, C., *Effects of S-Glutathionylation and S-Nitrosylation on Calmodulin Binding to Triads and FKBP12 Binding to Type 1 Calcium Release Channels.* Antioxid Redox Signal, 2005. **7**(7-8): p. 870-81.
52. Liu, Y., E.G. Kranias, and M.F. Schneider, *Regulation of Ca2+ handling by phosphorylation status in mouse fast- and slow-twitch skeletal muscle fibers.* American Journal of Physiology - Cell Physiology, 1997. **273**(6): p. C1915-C1924.
53. Uto, A., Arai, H., and Ogawa, Y., *Reassessment of Fura-2 and the ratio method for determination of intracellular Ca2+ concentrations.* Cell Calcium, 1991. **12**(1): p. 29-37.

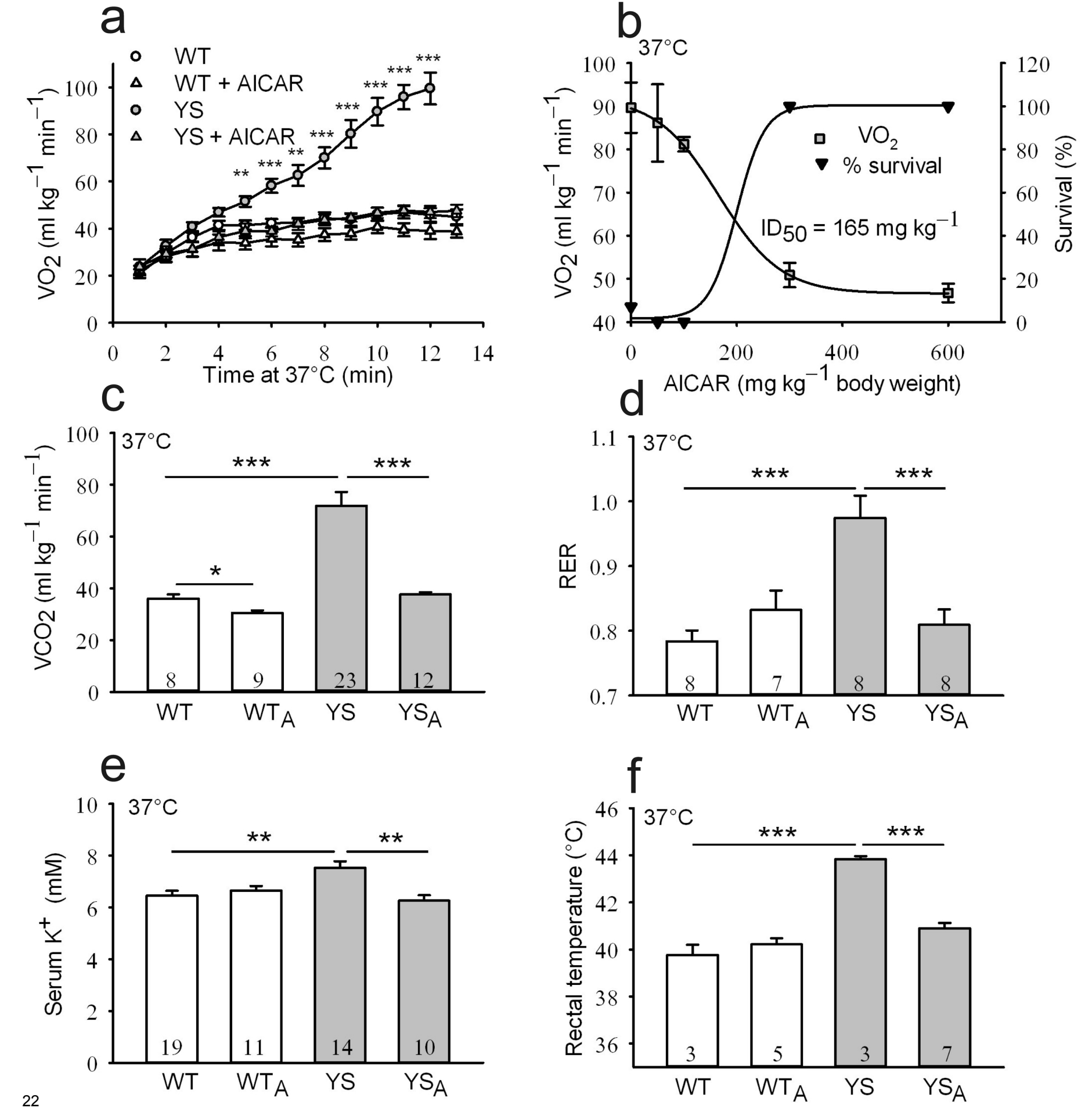
a
WT
WT + AICAR
YS
YS + AICAR
VO2 (ml kg−1 min−1)
Time at 37°C (min)
b
37°C
VO2
% survival
ID50 = 165 mg kg−1
VO2 (ml kg−1 min−1)
Survival (%)
AICAR (mg kg−1 body weight)
c
37°C
VCO2 (ml kg−1 min−1)
WT
WTA
YS
YSA
d
37°C
RER
e
37°C
Serum K+ (mM)
f
37°C
Rectal temperature (°C)

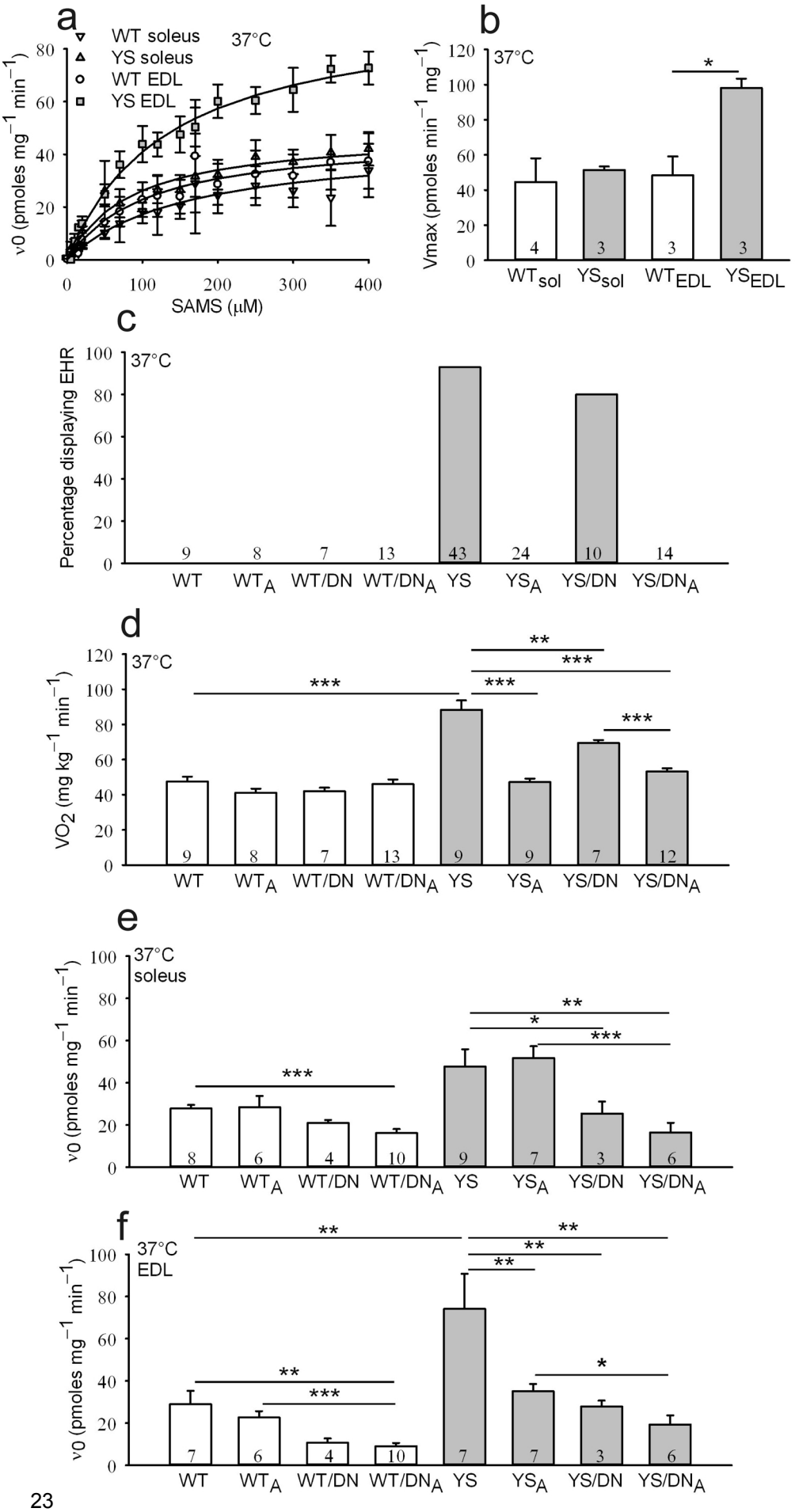
a
WT soleus
YS soleus
WT EDL
YS EDL
37°C
v0 (pmoles mg−1 min−1)
SAMS (μM)
b
37°C
Vmax (pmoles min−1 mg−1)
WTsol
YSsol
WTEDL
YSEDL
c
37°C
Percentage displaying EHR
WT
WTA
WT/DN
WT/DNA
YS
YSA
YS/DN
YS/DNA
d
37°C
VO2 (mg kg−1 min−1)
e
37°C
soleus
v0 (pmoles mg−1 min−1)
f
37°C
EDL
v0 (pmoles mg−1 min−1)

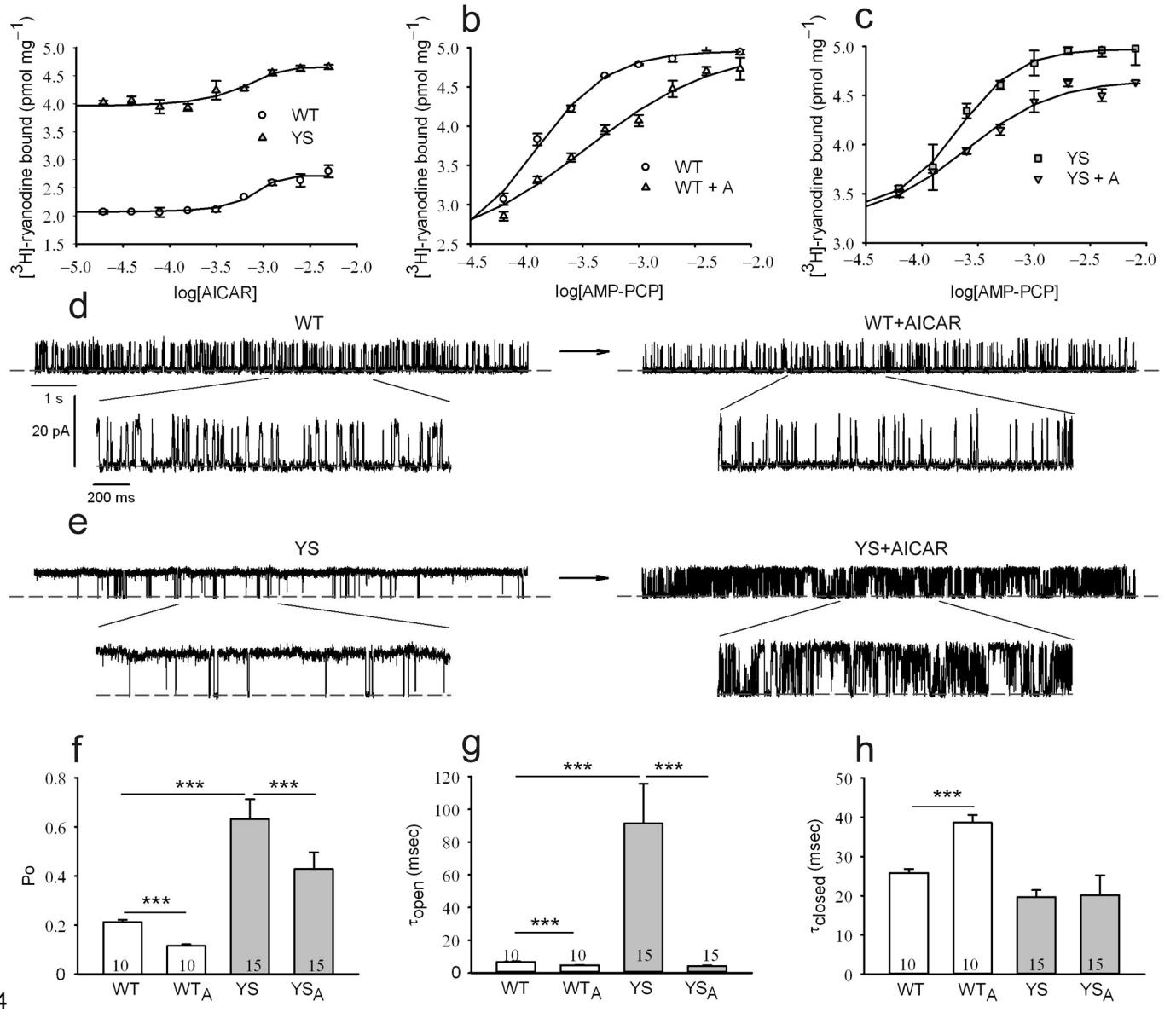
a
[3H]-ryanodine bound (pmol mg−1)
WT
YS
log[AICAR]
b
WT
WT + A
log[AMP-PCP]
c
YS
YS + A
log[AMP-PCP]
d
WT
WT+AICAR
20 pA
1 s
20 pA
200 ms
e
YS
YS+AICAR
f
Po
***
WT
WTA
YS
YSA
g
τopen (msec)
h
τclosed (msec)

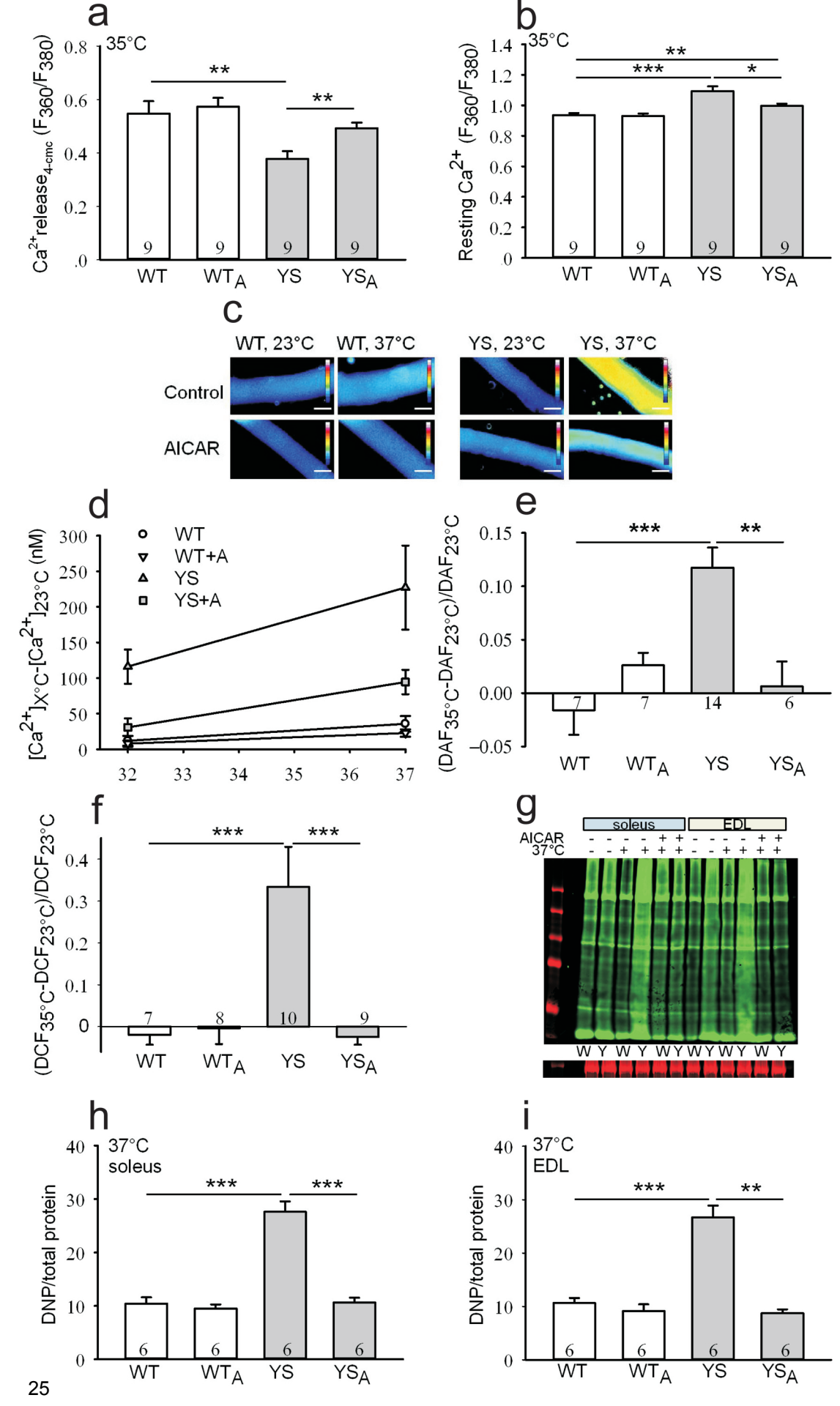
a
35°C
Ca^{2+}release$_{4\text{-cmc}}$ (F_{360}/F_{380})
0.8
0.6
0.4
0.2
.0
**
**
9
9
9
9
WT
WT_A
YS
YS_A
b
35°C
Resting Ca^{2+} (F_{360}/F_{380})
1.4
1.2
1.0
0.8
0.6
0.4
0.2
0
**
***
*
9
9
9
9
WT
WT_A
YS
YS_A
c
WT, 23°C
WT, 37°C
YS, 23°C
YS, 37°C
Control
AICAR
d
$[Ca^{2+}]_{X°C}$-$[Ca^{2+}]_{23°C}$ (nM)
300
250
200
150
100
50
0
WT
WT+A
YS
YS+A
32
33
34
35
36
37
e
($DAF_{35°C}$-$DAF_{23°C}$)/$DAF_{23°C}$
0.15
0.10
0.05
0.00
–0.05
***
**
7
7
14
6
WT
WT_A
YS
YS_A
f
($DCF_{35°C}$-$DCF_{23°C}$)/$DCF_{23°C}$
0.4
0.3
0.2
0.1
0
***
***
7
8
10
9
WT
WT_A
YS
YS_A
g
soleus
EDL
AICAR
37°C
W Y W Y W Y W Y W Y W Y
h
37°C
soleus
DNP/total protein
40
30
20
10
0
***
***
6
6
6
6
WT
WT_A
YS
YS_A
i
37°C
EDL
DNP/total protein
40
30
20
10
0
***
**
6
6
6
6
WT
WT_A
YS
YS_A

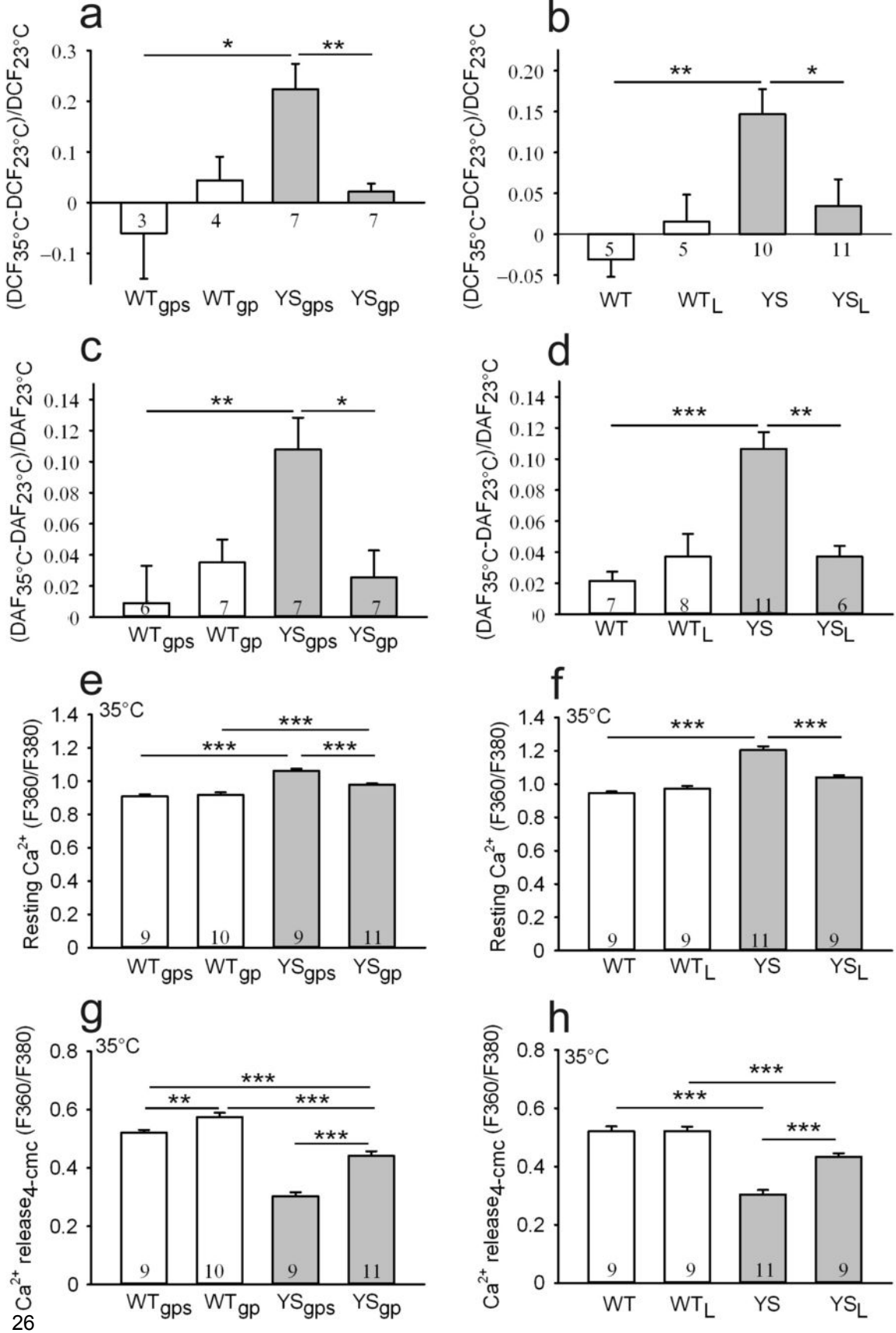
a
b
c
d
e
f
g
h
(DCF35°C-DCF23°C)/DCF23°C
(DAF35°C-DAF23°C)/DAF23°C
Resting Ca2+ (F360/F380)
Ca2+ release4-cmc (F360/F380)
35°C
WTgps WTgp YSgps YSgp
WT WTL YS YSL
*
**
***

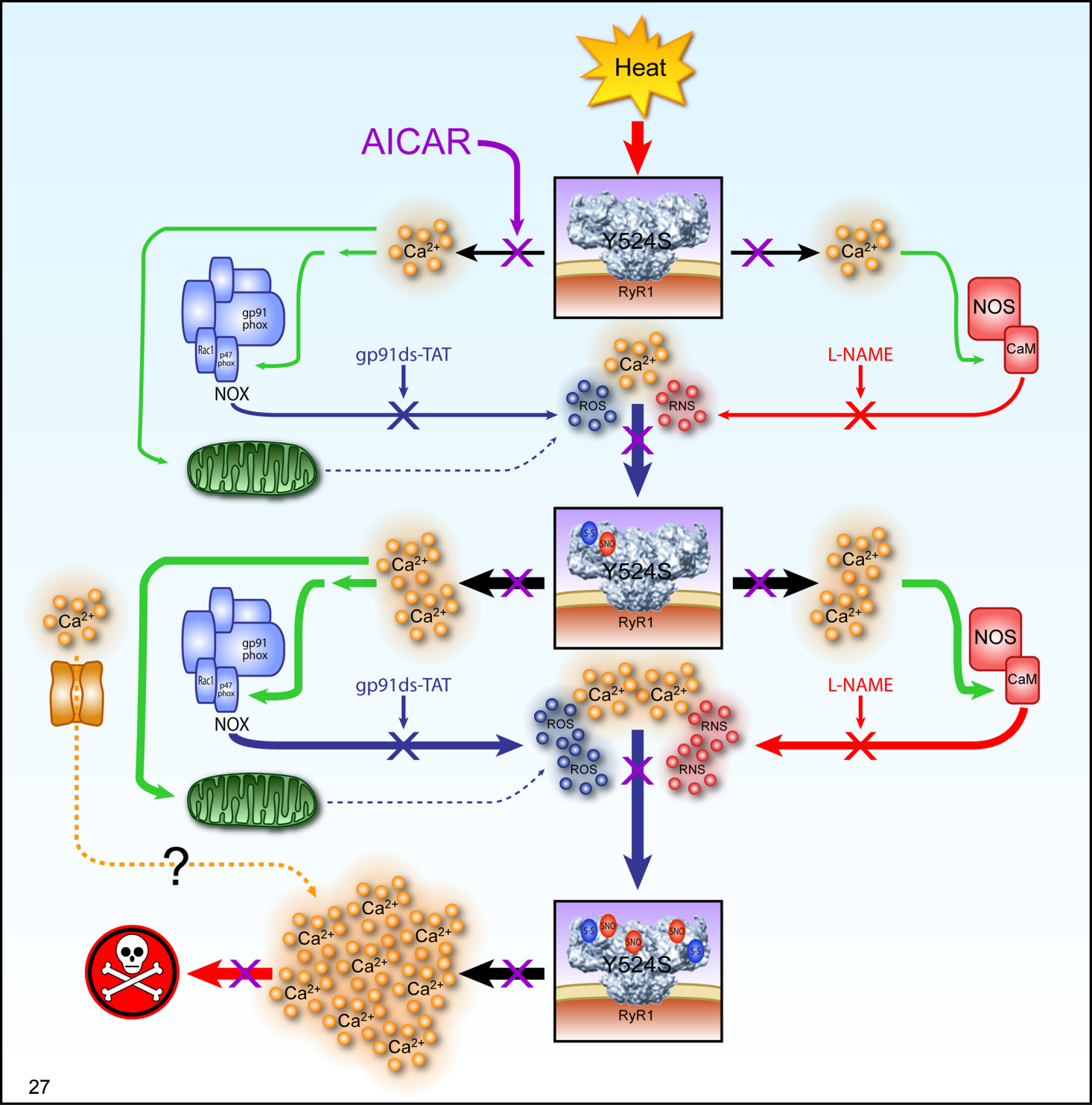
Heat
AICAR
Y524S
RyR1
Ca2+
gp91
phox
Rac1
p47
phox
NOX
gp91ds-TAT
ROS
RNS
L-NAME
NOS
CaM
S-S
SNO
?

AICAR Prevents Heat Induced Sudden Death in RyR1 Mutant Mice Independent of AMPK Activation

Johanna T. Lanner, Dimitra K. Georgiou, Adan Dagnino-Acosta, Alina Ainbinder, Qing Cheng, Aditya D. Joshi, Zanwen Chen, Viktor Yarotskyy, Joshua M. Oakes, Chang Seok Lee,Tanner Monroe, Arturo Santillan, Keke Dong, Laurie Goodyear, Iskander I. Ismailov, George G. Rodney, Robert T. Dirksen, and Susan L. Hamilton

Supplementary Table 1

	I-V data				(ΔF/F)-V data		
	G_{max} (nS/nF)	k_G (mV)	$V_{G1/2}$ (mV)	V_{rev} (mV)	$(\Delta F/F)_{max}$	k_F (mV)	$V_{F1/2}$ (mV)
WT	185 ± 12	5.8 ± 0.1	10.2 ± 1.2	65.2 ± 1.2	1.28 ± 0.15	5.3 ± 0.5	-6.1 ± 1.2
	n = 24	*n* = 24	*n* = 24	*n* = 24	*n* = 24	*n* = 24	*n* = 24
WT + 1mM AICAR	232 ± 14**	6.0 ± 0.4	12.1 ± 1.2	65.1 ± 1.7	1.34 ± 0.13	5.6 ± 0.4	-8.2 ± 1.0
	n = 24	*n* = 24	*n* = 24	*n* = 24	*n* = 24	*n* = 24	*n* = 24

Supplementary Table 1 Parameters of fitted I-V curves and ΔF/F-V. Values represent mean ± SEM from the number of myotubes indicated in *n*. G_{max} is the maximal L-channel conductance; $(\Delta F/F)_{max}$ is the maximal relative change in fura-2 fluorescence; V_{rev} is the L-channel reversal potential; $V_{G1/2}$ and $V_{F1/2}$ are the potential at which G and F are half maximal, respectively; k_G and k_F, are the slope factors for IV and FV, respectively. $^{**}P < 0.01$ compared to WT.

Supplementary Figure 1

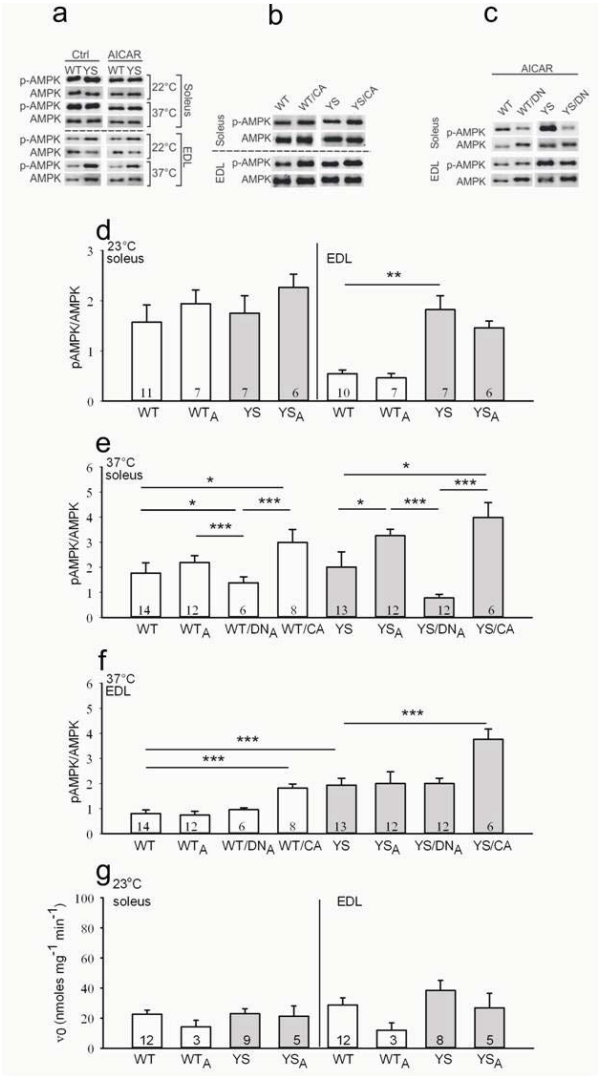

Supplementary Figure 1 Effect of AICAR on AMPK phosporylation. **(a)** Representative western blots of AMPK and pAMPK in muscles homogenates from mice treated with either 0.9% saline (Ctrl) or AICAR at 23 and 37 °C. (**b**) Representative western blots of AMPK and pAMPK in muscles homogenates from mice heat challenged at 37 °C. (**c**) Representative western blots of AMPK and pAMPK in muscles homogenates from mice injected with AICAR and heat challenged at 37 °C. (**d**) pAMPK/AMPK ratios, quantified by western blot analysis, in mice that have not undergone the heat challenge test. (**e**) pAMPK/AMPK ratio in the soleus and (**f**) EDL muscles of indicated mice and treatments. (**g**) AMPK activity in homogenates of muscles from mice exposed to room temperatures only (23 °C). AICAR treatment is indicated with the subscript A in panels d–g, the *n* numbers are also shown. **P* < 0.05, ***P* < 0.01, ****P* < 0.001.

Supplementary Figure 2

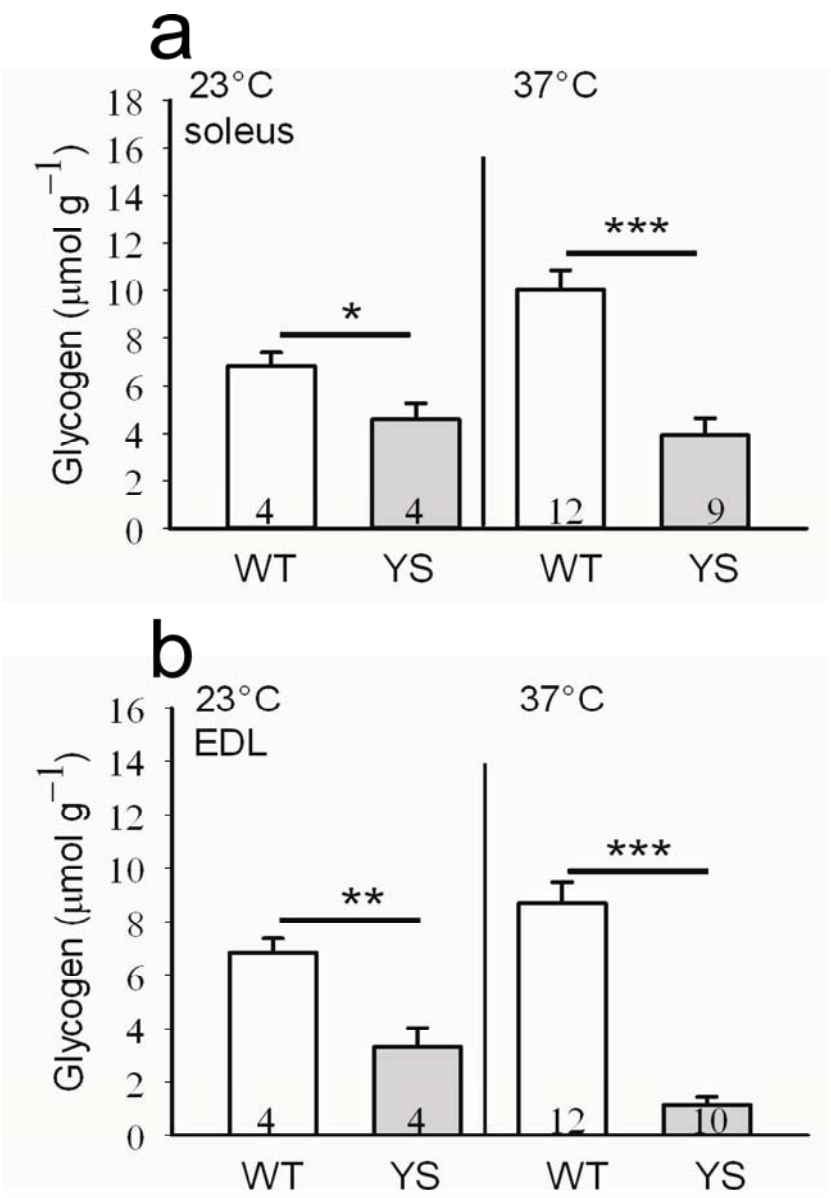

Supplementary Figure 2 Glycogen content. Glycogen of (**a**) soleus and (**b**) EDL muscles of genotypes and treatments shown, *n* numbers are indicated. **P* < 0.05, ***P* < 0.01, ****P* < 0.001

Supplementary Figure 3

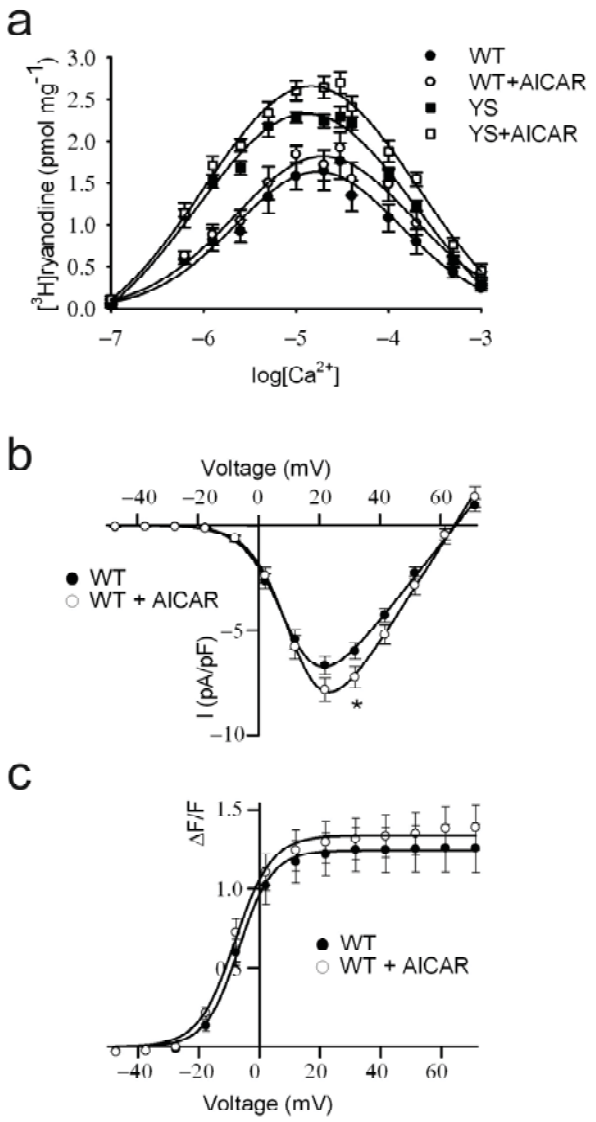

Supplementary Figure 3 Effect of AICAR on Ca^{2+} sensitivity of [^{3}H]-ryanodine binding and E-C coupling. (**a**) Representative plot of the effect of 1 mM AICAR on the Ca^{2+} sensitivity of [^{3}H]-ryanodine binding to sarcoplasmic reticulum membranes from YS and WT muscle. WT_{EC50}: 1.7 ± 0.2 μM, (*n* = 3); YS_{EC50}: 1.0 ± 0.1 μM, (*P* < 0.01) and WT_{IC50}: 190 ± 30 μM; YS_{IC50}: 190 ± 5 μM, (*n* = 3). Magnitude and voltage dependence of (**b**) peak L-type Ca^{2+} current density and (**c**) intracellular Ca^{2+} transients recorded in whole-cell clamp experiments in cultured myotubes in the absence or presence of AICAR (1 mM bath applied for 30 min), (*n* = 24), **P* < 0.05.

Supplementary Figure 4

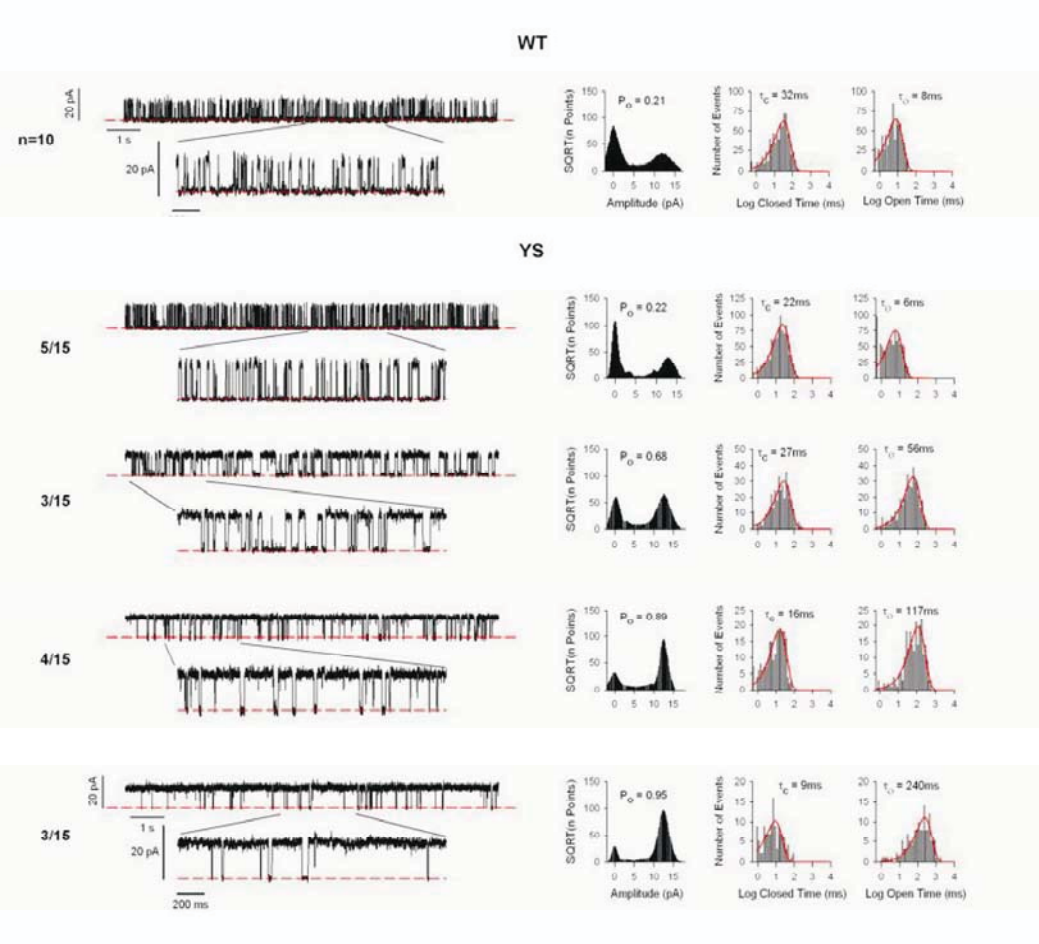

Supplementary Figure 4 Single channel activity of RYR1-WT and RYR1-YS channels reconstituted in planar lipid bilayers. Representative trace of a RYR1-WT channel and all point amplitude histogram, distributions of open and closed times of the channel (top). Representative traces of four subtypes of RyR1-YS channels grouped according to single channel kinetics (open probability, P_o) (bottom). Out of fifteen channels recorded, five had P_o of 0.23±0.02, three 0.66±0.03, four 0.87±0.04 and five 0.96±0.01. Plots next to the traces depict all-point amplitude and dwell-time analyses of each representative channel. Dashed red lines in the graphs correspond to closed state of the channels. Solid red lines in the dwell time histograms represent fits to a single exponential log probability function. All of these YS and WT channels were inhibited by AICAR in the presence of AMP-PCP. Channels with high (>10% of the time) sub-conductance behavior under basal conditions constituted ~40% of recordings (n = 11 out of 26), and were excluded from these quantitative analyses, as this is frequently a sign of damage of the channel during purification. However, in these channels, 1 mM AICAR also induced marked increases in preponderance of open/sub-conductance state(s), as compared to their respective baselines.

Supplementary Figure 5

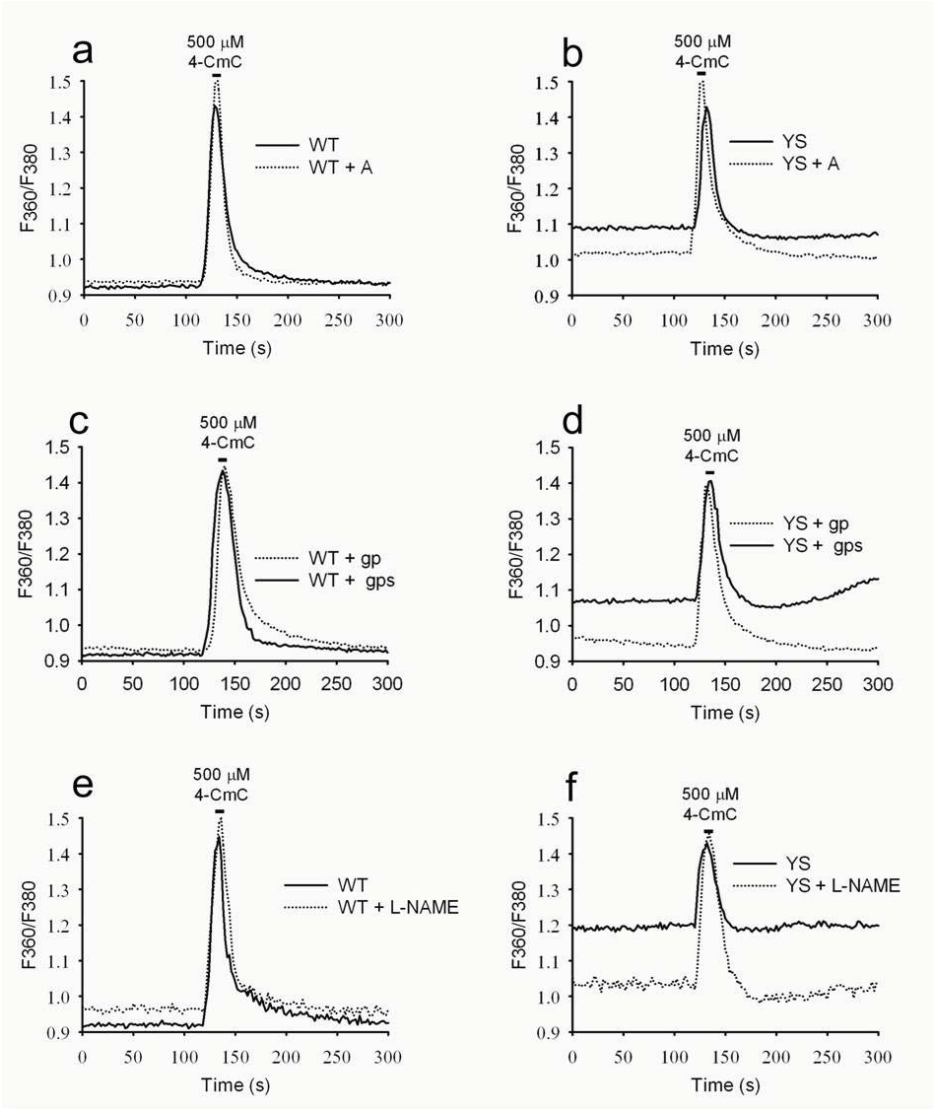

Supplementary Figure 5 Representative 4-CmC-induced $Ca2^{+}$ transients in single FDB myofibers. (**a**) Response of WT and (**b**) YS fibers in the absence or presence of bath applied AICAR (+A). (**c**) Response of WT and (**d**) YS fibers in bath applied gp91ds-tat (gp) or scrambled gp91ds-tat (gps) peptides. (**e**) Response of WT and (**f**) YS fibers in the absence or presence of bath applied L-NAME.

Supplementary Figure 6

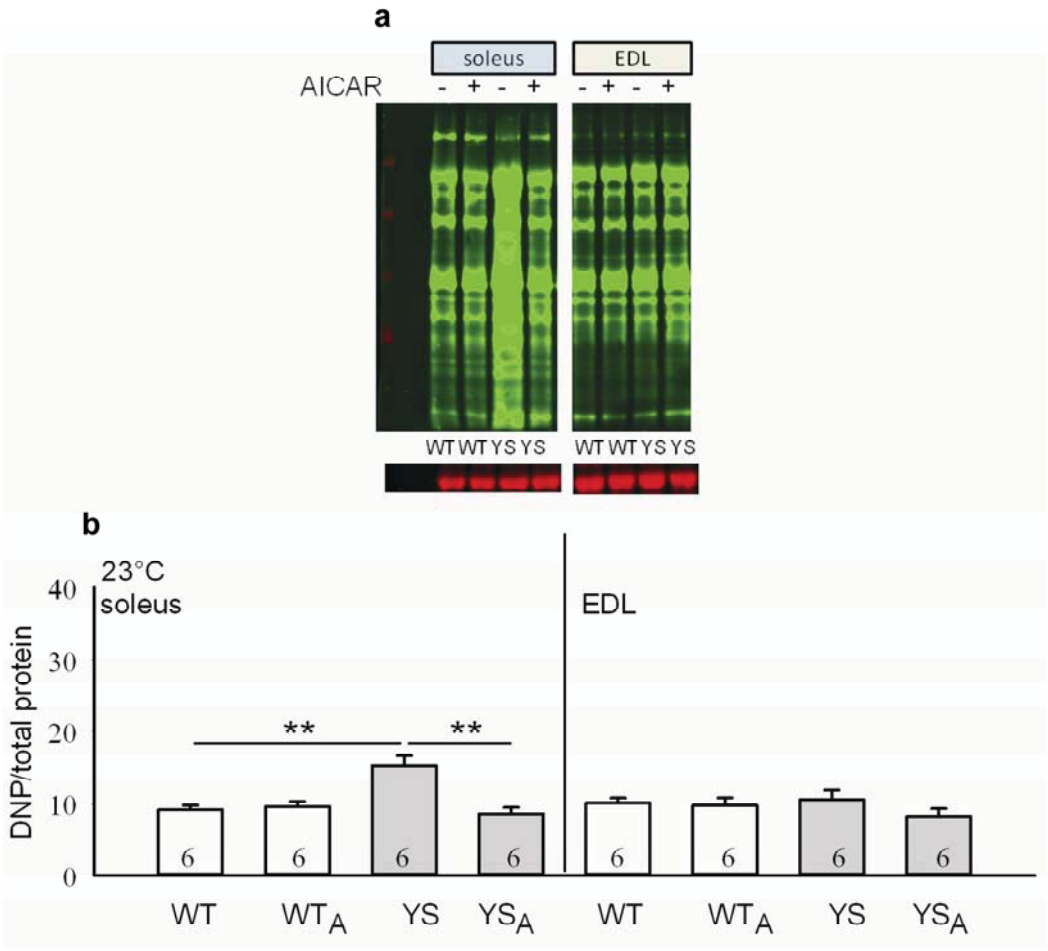

Supplementary Figure 6 Quantification of oxidative stress in muscle from mice at room temperatures. (**a**) Representative Oxyblot (top, pseudocolored green), and Coomassie stained non specific band (bottom, pseudocolored red). (**b**) Quantification of oxidative stress from the Oxyblots normalized to the non specific band. AICAR treatment is indicated with the subscript A, *n* numbers are also shown. $^{**}P < 0.01$

Supplementary Methods online

Muscle homogenates. We homogenized EDL and soleus muscles from WT and YS mice in ice-cold lysis buffer consisting of: 10 mM Tris pH 7.5, 1 mM EDTA, 1 mM Na_3VO_4, 10 mM $NaPyroPO_4$, 10 mM β-glyceophosphate, 10 mM NaF, 1% NP40 and proteases inhibitors. We used the Precellys tissue homogenizer and beads.

Western blot. We loaded equal amounts of total protein (15 µg) from crude homogenates to resolve by gel electrophoresis. We performed western blot analyses using pAMPK (1:1000, Cell Signaling), and AMPK-alpha (1:1000, Cell Signaling). LI-COR IRDye® infrared dyes were used as secondary antibodies and immunoreactive bands were visualized using the Odyssey Infrared Imaging System (LI-COR).

Ca^{2+} titration. Equilibrium ^{3}H-ryanodine binding (5 nM) was performed with skeletal muscle SR membranes as described[17] with or without 1 mM AICAR.

Glycogen. We measured muscle glycogen content of soleus and EDL muscles from WT and YS mice with the glucose assay kit (GAHK-20, Sigma) according to the instructions from the manufacturer.

ROS and RNS measurements. We placed the FDB fibers, plated on glass coverslides in the recording chamber (RC-21BDW, Warner instruments). We excited (0.5 Hz) the dyes (DCF or DAF) using a 500/20x nm filter (DG4) and recorded the emitted fluorescence (HQ560/80m). For DCF measurements, we collected the emitted fluorescence through a water immersion objective (40x0.7NA) coupled to a Nikon eclipse E600-FN upright microscope and digitalized with a CCD CoolSNAP HQ camera (394x1040 pixels field size, 0.16 mm/pixel and 8 bin resolution). For DAF measurements we collected the signal through an oil immersion objective (40x 1.3 NA) coupled to a Nikon eclipse TE200 inverted microscope and digitalized with a cascade 512B camera. We recored and analysed the data with the MetaFluor software (version 6.2).

The readily-releasable RyR1 Ca^{2+} pool and resting Ca^{2+}. We incubated the FDB fibers with 10 µM of the ratiometric Ca^{2+} indicator Fura-2AM (Invitrogen), in DMEM (Invitrogen) supplemented with 20 µM N-benzyl-p-toluene sulphonamide (BTS, TOCRIS) and 0.02% Pluronic F127 (Sigma) at 37 °C for 1 h, followed by a wash in a dye-free DMEM for 30 min. We excited fluorescence using a monochromatic light from a rapidly tunable galvanometric scanner-mounted grating (Polychrome IV; TILL Photonics), with a 150 Watt Xenon short arc lamp as a light source. We recorded pairs of images (100 ms exposure time) at the Ca^{2+}-sensitive wavelength (F1, 380 nm) and at the isosbestic wavelength (360 nm) through a 20x 0.5NA Achroplan W lens (Zeiss) at 2 sec intervals using an ORCA-R^2 CCD camera (Hamamatsu), mounted on an Axioscope 2FS equipped with a 400DCLP dichroic mirror and D510/40m emitter filter (Chroma Technology). We maintained the temperature of the bath solution (Tyrode solution, continuously

bubbled with 95%-5% O_2-CO_2, and perfused through the recording chamber at the rate of 2 ml min^{-1}) at 35 °C using a SF-28 in-line heater and a bipolar temperature controller TC344B (Warner Instruments). We acquired the data and controlled the monochromator via an Instrutech ITC-18 interface (HEKA) using a custom-developed software (kindly provided by Dr. Takafumi Inoue, Waseda University, Tokyo, Japan). We determined the content of intracellular Ca^{2+} stores as the integral of the changes in ratio of background subtracted Fura-2AM fluorescence in response to local application of 500 μM 4-CmC. We determined resting Ca^{2+} as a mean value of the fluorescence ratio in the first sixty consecutive images taken before application of 4-CmC. BTS was continuously present in the bath solution.

Fura-2 imaging in single FDB fibers. We loaded the FDB fibers with Fura-2 AM for 30 min at room temperature in Ringer's solution (146 mM NaCl, 5 mM KCl, 2 mM $CaCl_2$, 1 mM $MgCl_2$, 10 mM HEPES, pH 7.4). Fibers were then incubated for 30 min in dye-free Ringer's supplemented with either 25 μM 4-methyl-*N*-(phenylmethyl)benzenesulfonamide (BTS) or 25 μM BTS + 1 mM AICAR. Fibers were then placed in a temperature controlled chamber (Dagan, Corp., Minneapolis, MN) on the stage of an inverted epifluorescence microscope (Nikon Inc, Melville, NY) and alternatively excited at 340 and 380 nm (30 ms exposure per wavelength and 2 x 2 binning) using a monochromator-based illumination system. Fluorescence emission at 510 nm was captured using a high speed, digital QE CCD camera (TILL Photonics, Pleasanton, CA). Resting fura-2 ratios were obtained following >5 min equilibration at each three different temperatures: 23 °C, 32 °C and 37 °C for all fibers. Resting fura-2 ratios ($R = F_{340}/F_{380}$) for each temperature were generated and subsequently analyzed using NIH ImageJ software.

Measurements of depolarization-induced Ca^{2+} transients and L-type Ca^{2+} currents. Mouse primary skeletal muscle myotubes from at least three independent preparations were studied 4-7 days after differentiation and prepared as previously described [54]. Whole-cell L-type Ca^{2+} currents and intracellular Ca^{2+} transients were simultaneously recorded at room-temperature (21-23 °C) from myotubes derived from WT mice under conditions described previously[16,17,55,56]. Briefly, the external solution contained: 145 mM TEA-Cl, 10mM $CaCl_2$, 10 mM HEPES, pH 7.4, and the pipette internal solution contained: 145 mM Cs-aspartate, 0.1 mM EGTA, 1.2 mM $MgCl_2$, 0.2 mM K_5-Fluo-4 (Invitrogen, Eugene, OR), 5 mM Mg-ATP, 10 mM HEPES, pH 7.4. Cell capacitance was determined by integration of the capacity transient resulting from a +10 mV pulse applied from the holding potential (-80 mV) and was used to normalize Ca^{2+} currents (pA/pF) from different myotubes. Peak L-current density (pA/pF) was plotted as a function of membrane potential and fitted according to:

Equation 1. $I_{Ca} = G_{max} \bullet (V_m - V_{rev}) / (1+\exp[(V_{G1/2} - V_m)/k_G])$

where G_{max} is the maximum L-channel conductance, V_m is the test potential, V_{rev} is the reversal potential, $V_{G1/2}$ is the voltage for half-maximal activation of G_{max} and k_G is a slope factor. Relative changes in intracellular Ca^{2+} in patch clamp experiments were simultaneously recorded during each test pulse and

are reported as ΔF/F, where F is the baseline fluorescence immediately prior to depolarization and ΔF is the fluorescence change from baseline. Fluorescence amplitudes at the end of each test pulse were plotted as a function of membrane potential and fitted according to:

Equation 2. $\Delta F/F = (\Delta F/F)_{max} /(1+\exp[(V_{F1/2}-V_m)/k_F])$

where $(\Delta F/F)_{max}$ is the maximal fluorescence change, V_m is the test potential, $V_{F1/2}$ is the voltage for half activation of $(\Delta F/F)_{max}$ and k_F is a slope factor. Action potential induced Ca^{2+} transients and repetitive stimulation (10 min) were elicited by electrical field stimulation with a 0.1 Hz, 0.5 ms, 20 V pulse via a pair of platinum electrodes.

References

54. Beam, K.G., and Knudson C.M. J. Gen. Effect of Postnatal Development on Calcium Currents and Slow Charge Movement in Mammalian Skeletal Muscle. Physiol., 1988. **91**(6):781-798.

55. Tang, W. Ingalls, C.P., Durham, W.J., Snider, J., Reid, M.B., Wu, G., Matzuk, M.M., and Hamilton, S.L. Altered Excitation-Contraction Coupling with FKBP12 Skeletal Muscle Specific Deficiency. FASEB J, 2004. **18**: p.1597-9.

56. Long, C., Cook, L.G., Hamilton, L.S., Wu, G.Y., and Mitchell, B.M. FK506 Binding Protein 12/12.6 Depletion Increases Endothelial Nitric Oxide Synthase Threonine 495 Phosphorylation and Blood Pressure. Hypertension, 2007. 49(3): p. 569-76.